Accepted Manuscript

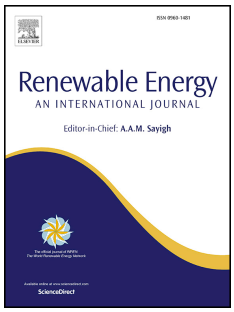

A large-scale renewable electricity supply system by 2030: Solar, wind, energy efficiency, storage and inertia for the South West Interconnected System (SWIS) in Western Australia

Dean Laslett, Craig Carter, Chris Creagh, Philip Jennings

PII: S0960-1481(17)30524-4

DOI: 10.1016/j.renene.2017.06.023

Reference: RENE 8887

To appear in: *Renewable Energy*

Received Date: 9 December 2016

Revised Date: 15 March 2017

Accepted Date: 4 June 2017

Please cite this article as: Laslett D, Carter C, Creagh C, Jennings P, A large-scale renewable electricity supply system by 2030: Solar, wind, energy efficiency, storage and inertia for the South West Interconnected System (SWIS) in Western Australia, *Renewable Energy* (2017), doi: 10.1016/j.renene.2017.06.023.

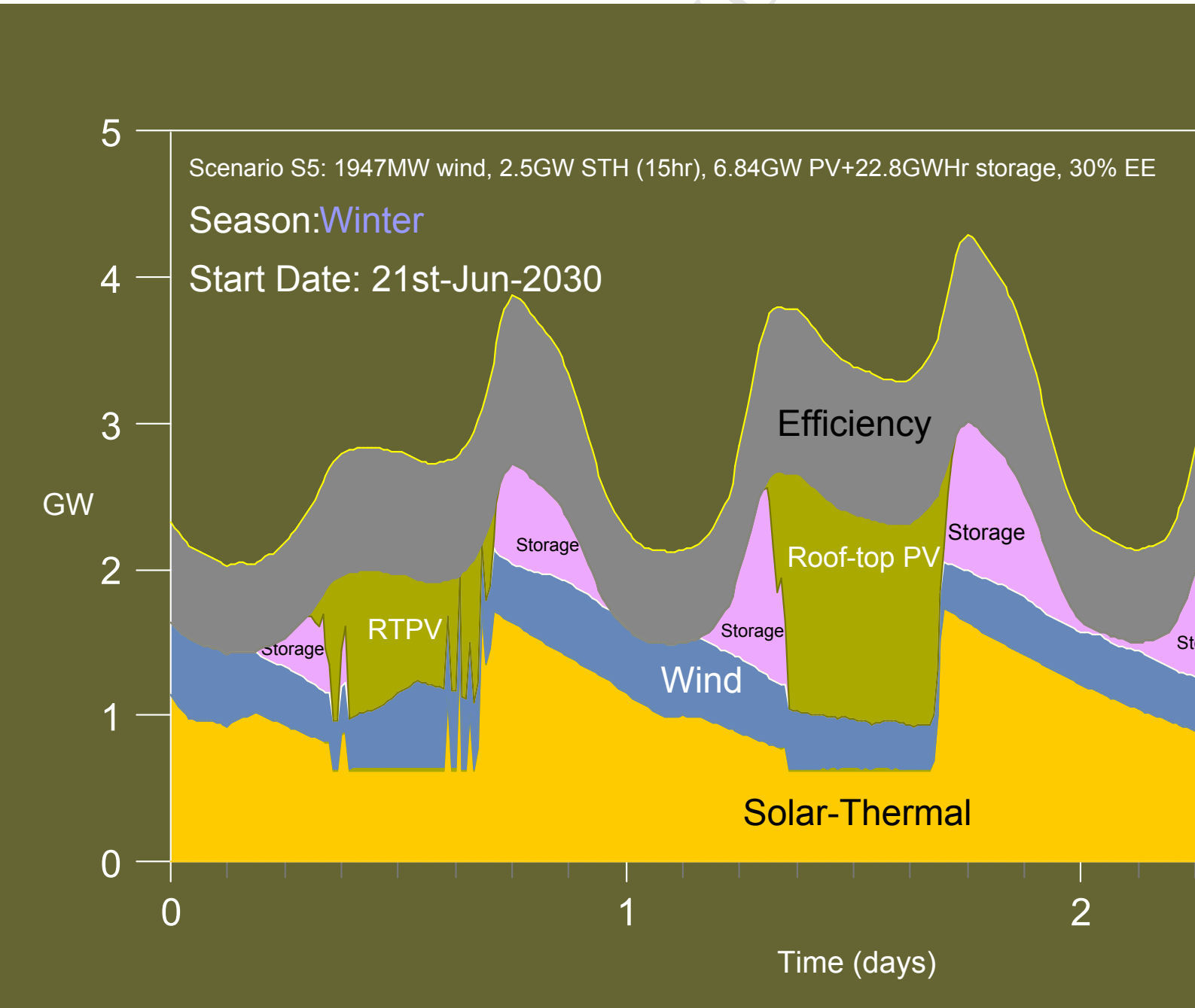
Scenario S5: 1947MW wind, 2.5GW STH (15hr), 6.84GW PV+22.8GWHr storage, 30% EE
Season:Winter
Start Date: 21st-Jun-2030
GW
5
4
3
2
1
0
0
1
2
Time (days)
Efficiency
Storage
RTPV
Storage
Storage
Roof-top PV
Storage
Wind
Solar-Thermal

A large-scale renewable electricity supply system by 2030: solar, wind, energy efficiency, storage and inertia for the South West Interconnected System (SWIS) in Western Australia.

Dean Laslett[a]*, Craig Carter[a], Chris Creagh[a], and Philip Jennings[a]

Murdoch University Western Australia

(a) School of Engineering and Information Technology, Murdoch University, South Street, Murdoch, WA 6150, Australia

*gaiaquark@gmail.com (Corresponding author)

Abstract

An interactive web tool was created to simulate 100% renewable electricity supply scenarios for the South-West Interconnected System (SWIS) in the south-west of Western Australia. The SWIS is isolated from other grids and currently has no available hydropower. Hence it makes a good case study of how supply and demand might be balanced on an hour-by-hour basis and grid stability maintained without the benefit of energy import/export or pumped hydroelectric storage. The tool included regional models for wind and solar power, so that hypothetical power stations were not confined to sites with existing wind farms or solar power stations, or sites with measurements of wind speed and solar radiation. A generic model for solar thermal storage and simple models for energy efficiency, distributed battery storage and power to gas storage were also developed. Due to the urgency of climate change mitigation a rapid construction schedule of completion by 2030, rather than the more common target of 2050, was set. A scenario with high wind generation, and scenarios with varying levels of solar power, wind power, distributed battery storage, energy efficiency improvements and power to gas systems were considered. The battery storage system and PV arrays were configured to provide synthetic inertia to maintain grid stability (with a small loss in capacity for each), and existing synchronous generators were kept spinning with no fuel input, adding a small increase to the electrical load demand. The level of synthetic inertia provided by battery storage was estimated for each scenario. The results indicated that a balanced mix of solar PV, solar thermal, efficiency, and storage were the most feasible to be built on a rapid time scale. The required capacity and build rate of the generation and storage systems would be reduced if energy efficiency improvements were implemented on a more rapid schedule compared to the current global improvement rate. The scenario with very high

levels of wind power (~80% generation) were found to be capable of meeting SWIS reliability criteria if very large amounts of distributed storage or some high capacity seasonal reserve generation system such as power to gas were present. High levels of battery storage capacity and efficiency improvement could be as effective as a power to gas system. It was confirmed that all scenarios provided the same or greater levels of inertia than presently provided by conventional generators. This tool showed that it is possible to examine renewable energy scenarios for regional electricity networks without high computing power.

Keywords: 100 percent renewable energy simulation; Energy efficiency; Solar thermal power tower energy storage model; Power to gas storage.

1. Introduction

There is a growing realisation that limiting global temperature rise to 2°C above pre-industrial levels may not be a safe limit, and that 1.5°C is more appropriate [1]. The recent Paris agreement on climate change specifically emphasised the need to hold the global average temperature rise to well below 2 °C and pursue efforts to limit the rise to 1.5 °C [2]. The number of climate related human deaths by the year 2050 has recently been estimated to be around half a million [3]. Thus the need to cut greenhouse gas emissions deeply is becoming increasingly urgent. Currently electricity generation is one of the major emission sources because of our heavy reliance on fossil fuels. Ways are now being found to meet electricity service needs without high emissions, typically by using forms of renewable energy and improving energy efficiency. The most well known example of a whole country being supplied with electricity almost solely from low emission sources is Iceland, which has large scale geothermal and hydroelectric resources. Other countries that supply a large part of their electricity demand from hydroelectric resources are Uruguay, Bhutan, and Albania [4]. There have also been a number of scholarly articles published that use measured renewable energy resource data at specific locations to simulate how the large-scale electrical or total energy needs of a country, state, or region might be supplied using renewable energy generation systems on an hour-by-hour basis (eg Barrett [5], Blackburn [6], Budischak et al. [7], Connolly et al. [8], Connolly et al. [9], Elliston et al. [10], Jacobson et al. [11], Herbergs et al. [12], Hoste et al. [13], and Lehmann et al. [14]). 100% renewable electricity might be defined as meeting all electrical demand using generation from renewable energy over an extended timespan, such as one year. Elliston et al. [10] developed 100% renewable electricity scenarios for the East coast of Australia. To a greater or lesser extent, many of these studies rely on large-scale hydroelectricity and energy imports and exports to balance supply with demand.

Hydroelectric and geothermal resources or imports from other grids may not be available on a large enough scale in many countries or regions. Instead, the available renewable energy resources are likely to be spatially and temporally variable in nature, such as sunshine and wind, and the demand also varies with time. Variable renewable energy generation is already gaining a significant presence in world electrical grids. However, to be a viable option on a global scale for eliminating nearly all greenhouse emissions, variable resources such as wind and solar must be able to go all the way, and supply 100 percent of the electricity needs of a large industrial economy. Supply and demand must be balanced on an hourly, daily, and seasonal basis, while maintaining grid stability on sub hourly time scales.

The use of energy storage technologies has been identified as having great potential to complement variable renewable energy systems and help them meet this challenge [15]. Weitemeyer et al. [16] found that for Germany, storage was needed above 50% generation by wind and solar, and seasonal storage was needed at generation levels above 80%. The use of an integrated energy supply approach, where heating, cooling and transport energy demand are included along with electrical demand, and energy can be switched between all three forms and stored, is also considered to enhance the potential for utilisation of variable renewable energy sources [17], [18], [19]. Although this study concentrated on the electrical demand only, the integrated energy approach can be utilised through what is commonly termed Power to Gas (P2G). Electricity is converted to a fuel, such as hydrogen or methane, for long term storage, and then reconverted back to electricity by burning the fuel in gas turbines, or by some other process [20]. Although the round trip efficiency is very low compared to other storage systems, the storage capacity is very high, so this approach may also have the potential to provide a seasonal storage system [16], and thus reduce the capacity required to be built in order to generate enough electricity during seasons of low wind and solar availability [21]. However, although a few pilot plants are in operation, this technology has yet to be used on a large scale and requires further technical and economic development [22]. In arid and semi arid regions, water consumed by the power to gas process could be a significant constraint, although seawater has been used as a source [22]. A portion of the water used in the P2G process can also be recycled [23], and if the P2G plant is close to a gas turbine power plant, then the CO_2 emitted can be fed back into the methane conversion process. However, steps must be taken to minimise leakage of stored methane, itself a potent greenhouse gas, to the atmosphere.

This study took a further step towards demonstrating the viability of variable sources by simulating how solar and wind energy might supply the South West Interconnected System (SWIS) on an hour-by-hour basis, while maintaining stability. The SWIS is an electric grid that supplies the South-West region of Western Australia (SWWA), and is a relevant case study because it is isolated from all other grids and does not currently have access to large-scale hydroelectric resources. Hence it is particularly dependent on 'spinning

reserve' being provided by fossil fuel generation to maintain stability [24]. Spinning reserve refers to reserved excess capacity of high inertial mass generators that spin in synchronisation with the grid. The reserved capacity is not used until required. Around 317 MW of spinning reserve was maintained on the SWIS grid in 2013 [25].

The SWIS is made up of a transmission network and a number of sub-transmission and distribution networks. The present configuration of energy generation systems connected to the SWIS is dominated by conventional fossil fuel power stations, with about 1600 MW of coal fired generation capacity, 1640 MW of gas fired generation capacity, and a further 1310 MW of mixed gas and liquid fuel generation capacity [26]. The main load centre is the city of Perth, which is connected to three main transmission line corridors (see Figure 2). The SWWA region also has an extensive gas supply and storage network [27], part of which is used to fuel the existing gas turbine generators.

The word 'dispatchable' is commonly used to represent flexible generation systems which can adjust output according to demand, and 'non-dispatchable' to those that are variable and cannot adjust upwards to meet demand, such as wind and solar. Conventional coal fired power stations are considered to be dispatchable, but have a required minimum operational power output level. If output is below this level, they must either shut down completely to avoid damage or operate at reduced efficiency. In reality, any generation system will have a degree of dispatchability (either more or less), that might differ over different time scales. Conventional power plants also often have a maximum sustainable ramp rate, which is a measure of how fast the power output can change (either rising or falling). Exceeding this rate could lead to higher maintenance costs or damage to the plant. In general, dispatchable generators are expected to respond to changes in the output of non-dispatchable generators and changes in demand to balance the system.

Conventional grids have traditionally relied on synchronous generators with a large rotational inertia for frequency stability control and fast voltage regulation for voltage stability and control. The inertia determines the initial rate of change of frequency in response to sudden changes in generator loading, before the primary and secondary stability control systems activate. The larger the inertia, the smaller the rate of change of frequency. The primary stability control systems attempt to arrest the frequency change, while the secondary control systems attempt to return the frequency to its reference value. Riesz et al. [28] estimated that there was around 12400 MWs of inertia on average in the SWIS grid, provided predominantly by conventional fossil fuel power plants. These power plants would be retired under a 100% renewable energy scenario, leading to a large reduction of inertia in the system. Therefore alternate means must found to maintain frequency and voltage stability. One possible option is to retain some of the existing synchronous generators and keep them spinning but disconnected from their rotational energy source ('de-clutched'), in

effect acting as synchronous compensators with no fuel input. There would be a cost however. Power losses in these generators could be up to 2% of their rated power [29].

Batteries and photovoltaic systems can provide voltage control but have no intrinsic rotational inertia. However, there are ways in which they could provide fast responding active frequency stability control to compensate for the reduced system inertia. Battery storage systems have a very rapid response rate and can provide frequency stability capability, if they are maintained in a partially charged state [30]. They can also provide 'synthetic rotational inertia' or 'inertia mimicking' [31]. The findings of Knap et al. [32] suggested that the inertia constant of lithium ion batteries is at least 50 MWs per MW of output power.

PV systems can already respond to increases in system frequency by decreasing generated power. They can also be deliberately operated at less than their maximum potential power at any one time, as determined by the solar irradiance. These 'de-loaded' PV systems can thus increase their generated power in response to decreasing system frequency [33]. Thus standalone PV systems could provide extra synthetic inertia during times of peak demand, but not at night.

The rotating generators of solar thermal power stations can also provide inertia. However on the SWIS most solar thermal stations are likely to be far from the main load centre (the greater Perth metropolitan area). If there is no central source of inertia, then the risk of these remote generators losing synchronism with one another increases. Wind turbines can be configured to provide synthetic inertia, and can more easily recover from faults or disturbances that could cause loss of synchronism. However, the risk of faults or disturbances in the grid isolating a wind farm (and its synthetic inertia) from the main load centre increases with longer transmission distances.

Vidal-Amaro et al. [34] considered grid stability for high penetration (although not 100%) renewable energy scenarios. However, absent in many previous 100 percent renewable generation simulation studies is consideration of the potential threat to system stability from loss of inertia as conventional generators are replaced by renewable energy systems. As a consequence, possible increases in the required installed capacity of renewable energy and storage technologies, in order to deploy systems to mitigate the potential for instability, are not accounted for. In this study, systems to maintain stability were implemented, and integrated into each 100% renewable energy scenario. The inertia for each scenario was estimated and compared to the 12400 MWs of inertia in the current SWIS system. It was not the intent of this study to model grid stability in detail. Rather, in assessing how much renewable energy, storage and reserve capacity is required to supply 100% of electrical demand hour by hour, it is important that the requirements for grid stability on shorter time scales are also met.

Changing a large-scale fossil fuel dominated electricity system to run on renewable energy cannot happen overnight. While many global emission reduction studies set a target year of 2050 [35], the urgency to reduce emissions means the transition should happen more quickly. Therefore this study investigated scenarios for reliably supplying the SWIS grid with 100% renewable energy and energy efficiency by the year 2030. The required installation rate of each technology to implement such a system within this time frame was estimated, while also taking into account population growth. To be a feasible option for rapidly reducing emissions and making the SWIS 100% renewable, the required capacity for each technology must be moderate enough such that it can be installed within this short time scale. The potential of power to gas seasonal storage systems to reduce the required build was also examined.

Onshore wind farms and solar photovoltaic (PV) systems were the main solar and wind technologies chosen here because these technologies are already in global large scale commercial operation, have falling costs, and as of 2015, there is already about 460 MW of onshore wind capacity and almost 500 MW of roof top solar PV capacity connected to the SWIS. Solar thermal technology was also considered. Although not as mature as wind and solar PV, it is in smaller scale commercial operation globally, has storage capability and is considered to have a high ramping capability [36]. These characteristics make solar thermal plants dispatchable [37]. Distributed battery storage is modelled because there is already uptake of batteries by households and businesses. Improvements in energy efficiency, that reduce demand, were also considered to be integral to any renewable energy system.

Although costs are not explicitly considered here, the costs of wind power and solar PV have fallen rapidly over the past decade, to the point where new build wind power in particular can compete with new build fossil fuel power stations. Mathiesen et al. [38] found that 100 percent renewable energy systems may be economically beneficial compared to fossil fuel systems. The costs of solar thermal stations are currently higher, as they are not as far along the development curve. However, Elliston et al. [39] found that the cost of a 100% renewable energy system for the national grid in Eastern Australia, including solar thermal stations, was competitive with fossil fuel based low carbon alternative systems, so a similar finding is plausible for the SWIS in Western Australia. Riesz et al. [40] found that the lowest cost renewable energy system scenarios for Australia had very high levels of wind power generation. The feasibility of such a scenario for the SWIS was investigated in this study.

2. Method

An interactive web based design tool was developed to enable a number of power supply system scenarios to be constructed and analysed. Models for generation of synthetic hourly values for solar radiation and

wind power for all seasons and for any location in the South-West of Western Australia have been developed previously by the authors [41] [42]. A simple model for solar thermal power generation with thermal storage was developed in this study, as it is considered to be a low emission technology that has rapid response rates. Simple models for home battery storage and energy efficiency were also developed, as these could have a significant future presence in the SWIS. All of these models were integrated into the design tool, hence scenarios could be constructed with different configurations of solar PV, solar thermal, and wind power stations, placed at various locations throughout the south-west of Western Australia, along with distributed storage and energy efficiency measures. Interactivity was achieved by coding all models in the commonly used World Wide Web page languages of Javascript and Dynamic HTML, such that the overall simulation could be run inside a web browser.

Hourly values for solar radiation were generated at each location where a solar power station was placed, and hourly values for hub-height wind speed were generated at each location where a wind farm was placed. To translate these values into power generation, the behaviour of the energy collection and generation device at each location was modelled. For each scenario in the simulation, the amount of non renewable energy generation required for each hour was calculated using:

$$nonre = Load_{y,h} - EE_h - P_{out,storage} - glf_{rtpv} P_{out,rtpv} - \sum_{n=1}^{n_{large}} glf_n P_{out,n} \quad (1)$$

where *nonre* is the non-renewable power generation (MW), $Load_{y,h}$ is the simulated hourly baseline SWIS load demand at hour h for year $y \geq 2009$ (MW). EE_h is the load demand reduction at hour h due to any energy efficiency measures, if implemented (MW). $P_{out,storage}$ is the output power from distributed storage, if present on the grid (MW). $P_{out,rtpv}$ is the total output from rooftop solar connected to the grid (MW). glf_{rtpv} is the grid loss factor for distributed rooftop PV generation. glf_n is the grid loss factor for large power station n. n_{large} is the number of large-scale renewable power stations on the system. $P_{out,n}$ is the output power for each station (MW). Each large power station could be modelled as a fixed PV array, a wind farm, or a solar thermal farm. If distributed storage is implemented in a scenario, then the simulation attempts to adjust $P_{out,storage}$ so that *nonre* is zero.

Publicly available half hourly demand data for the SWIS over seasonal time scales were aggregated into average hourly values. The total SWIS load demand for every hour throughout the year of 2009 was used as a baseline for the load demand profile (for typical summer and winter daily profiles, see Figure 1). The year

2009 was chosen because after that time significant amounts of distributed roof top solar generation began to be connected to the grid, reducing daytime demand. The effect of future population increase on baseline power demand was modelled by multiplying the 2009 load demand by a factor reflecting compounded yearly population growth:

$$Load_{y,h} = Load_{2009,h}\left(1+\frac{pop}{100}\right)^{(y-2009)} \quad (2)$$

where $Load_{y,h}$ is the load profile for year y at hour h (MW), $Load_{2009,h}$ is the 2009 profile at hour h (MW), and pop is the percentage yearly population increase. pop was set to a value of 2% per year, reflecting the average growth rate of Australian greater capital cities from 2013 to 2014 [43]. y was set to 2030 to establish the implementation target year.

To assess whether complete renewable energy generation had been achieved, 100 simulation runs under typical weather conditions were carried out for each scenario, and the maximum shortfall in renewable energy generation compared to the load was recorded. Two SWIS reliability standards were used to access the shortfall. The first reliability standard was taken to be a 0.05% loss of load probability (LOLP), here estimated as the fraction of time that renewable energy generation fell short of the load demand [44]. The second standard was a 0.002% shortfall in generated energy over one year. Renewable energy generation capacity was added to each scenario until these standards were met for 95 runs out of 100.

Transmission losses

To model generation from regional power stations, transmission losses between the stations and the load were estimated. In the SWIS system, the city of Perth is the major load centre. To approximate the losses incurred when transporting power through the grid, it was assumed that all electricity generated by each power station travelled to Perth. Up-conversion losses from each power station to the grid, and down-conversion and distribution losses to the loads were each modelled as a set power percentage loss. The backbone of the SWIS grid was modelled as having several links (Figure 2). Any new power station added to the system attached a new grid link from the power station to the nearest backbone link. All new links were assumed to use High Voltage Alternating Current (HVAC) technology, to allow easy interconnection with the existing HVAC grid.

Although cross-conversion losses between one grid link and another are likely to be lower than the up-conversion losses, they were assumed to be similar for modelling simplicity. Transmission losses were represented as a power percentage loss per 1000 kilometres of transmission line. The electricity generated by a power station would typically travel over several grid links before reaching Perth. For a power station n, $1 \le n \le n_{large}$, the total grid loss was estimated using:

$$glf_n = (1 - 0.01\,ld)\{\prod_{i=0}^{nlink_n - 1}(1 - 0.01\,lup_i)\}\{\prod_{j=1}^{nlink_n} e^{(-\frac{tl_j d_j}{10^5})}\} \quad (3)$$

where $nlink_n$ is the number of links travelled before reaching Perth, ld is the percentage down-conversion and distribution loss, lup_i is the percentage up-conversion loss from the power station when i=0 and the cross-conversion loss between grid link i and grid link i+1 when $i > 0$, tl_j is the percentage transmission loss per 1000 km for grid link j, d_j is the length of grid link j (km) and glf_n is the total grid transmission factor (the fraction of power that reaches the end users in Perth) for the power station. glf_n will be different for each power station, depending on its location, proximity to Perth, and which grid links the electricity travels through. The values used for each parameter are given in Table 1 below:

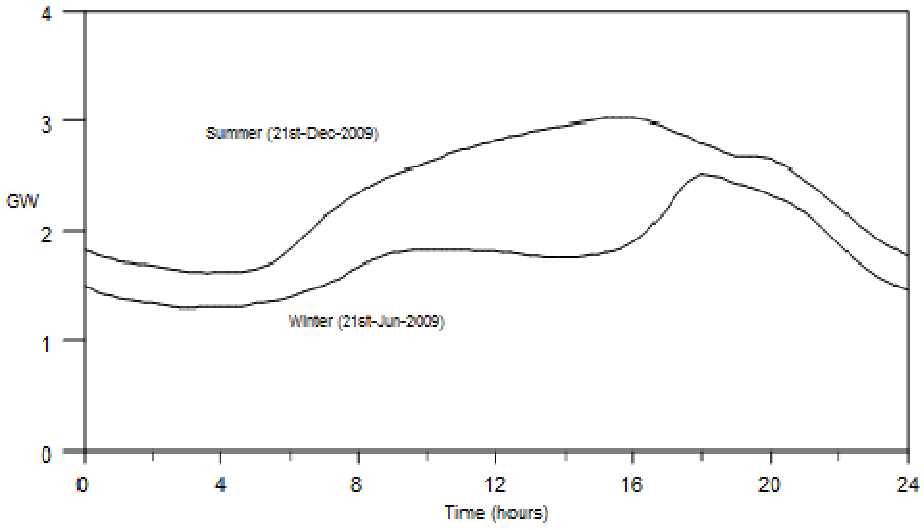

Figure 1. Typical summer and winter daily load profile on the SWIS grid for the year 2009.

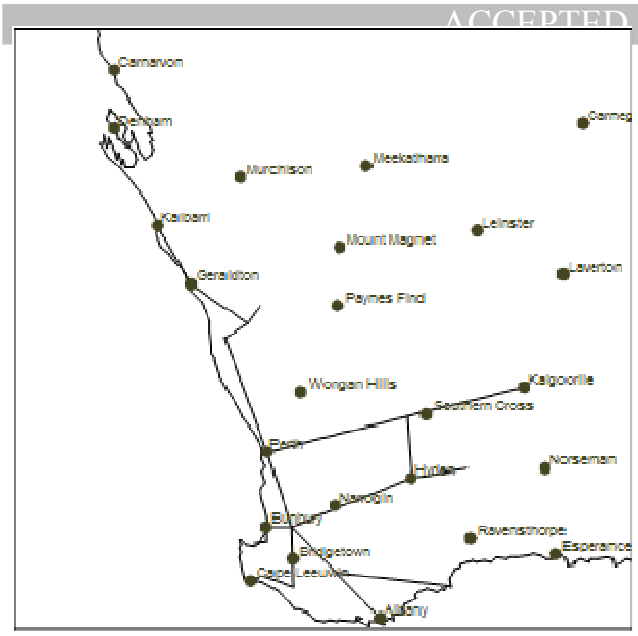

Figure 2. SWIS grid backbone links used by the model.

Table 1. Grid conversion and transmission loss parameters.

Parameter	Description	Value
lup	Up-conversion and cross-conversion loss (%)	0.62[a]
ld	Step-down and distribution loss (%)	9.5[b]
tl	Line loss (% per 1000 km)	6.93[c]

[a]Negra et al. [45]. [b]Dortalina and Nadira [46] and Masoum et al. [47]. [c]Bahrman [48].

Roof top solar PV was assumed to be scattered throughout the Perth distribution network and was subject to an 8% up-conversion and distribution loss on average [49], such that $glf_{rtpv} = 0.92$. 2034 MW of existing gas or mixed fuel gas turbines situated near Perth were also retrofitted or configured to operate in synchronous compensator mode, with the gas turbines de-clutched from the synchronous generators, which have some rotational inertia. This was to provide a stable frequency reference near the load centre for the more distant generators to synchronise with, and back-up generation capacity in case of generator failures or shortfalls during periods of sustained low solar and wind availability. There is usually no fuel input to the turbines, and the extra continuous load required to keep the back-up generators spinning was estimated to be about 41 MW, assuming power losses in these generators were 2% of the rated power.

Solar PV model

The global solar irradiance, I_g, is the total solar power per unit area falling on a flat surface and can be divided into three components: beam (also called direct), diffuse, and reflected. The beam component has come directly from the sun, the diffuse component results from radiation that has been scattered in the atmosphere, and the reflected component results from radiation reflected off other surfaces. The diffuse and reflected components are indirect, and they have a complex relationship with the beam component, depending on clouds and atmospheric conditions.

The generation of synthetic values of hourly average global solar irradiance at a particular location was based on calculation of the clear-sky beam normal irradiance, which is the beam irradiance falling on a surface perpendicular to the direction of the sun. The clear-sky diffuse and reflected components were then estimated from the clear-sky beam normal irradiance (the reflected component is usually negligible). To model the effect of clouds, all three components were modified according to an hourly "cloudiness" value that affects the amount of direct, diffuse, and reflected sunlight reaching the Earth's surface. The cloudiness values were generated randomly using a first order autoregressive algorithm, meaning that there was some dependence on the cloudiness value of the previous hour. The statistical properties of the cloudiness values were adjusted for location by calibration to measured data at 31 separate meteorological stations, and also adjusted to reflect seasonal changes. See Laslett et al. [41] for a detailed explanation of these parameters. The average Mean Bias Error (MBE) between the synthetic and measured irradiance falling on a horizontal plane was found to be -0.81%, indicating slightly conservative synthetic values. The monthly averaged irradiance Root Mean Square Error (RMSE) was 10.5%. PV systems can generally use all three components of solar radiation, but a fixed PV panel will not always be orientated perpendicular to the position of the sun as it moves through the sky, so the irradiance was recalculated each hour accounting for the changing angle of incidence between the sun and the panel.

An ideal solar cell has a power output that is linearly proportional to the global solar irradiance I_g. The performance ratio (PR) is a measure of how well a cell performs compared to an ideal cell [50]:

$$PR = \left(\frac{P_{out}}{P_{rated}}\right)\left(\frac{I_g}{1000}\right) \quad (4)$$

where P_{out} is the electrical output power (W), P_{rated} is the rated output (W) and I_g is measured in Wm^{-2}. Carr and Pryor [50] tested a number of cells in the Perth area and found PR values ranging from 0.79 to 0.93, with the highest values occurring during winter. The efficiency of solar cells has been found to decrease with

lower global irradiance and higher temperatures. To model this behaviour for fixed axis PV power stations and rooftop PV arrays, cell efficiency drop off was approximated by using an empirical expression for P_{out}:

$$P_{out}(I_g, DOY, h) = \left\{\frac{16250 + I_g^2}{25000 + I_g^2}\right\} \frac{I_g}{1000} \left\{1 - \frac{0.17}{4}(1+\cos(\frac{2\pi}{365}(DOY - 16)))(1+\cos(\frac{2\pi}{24}(h - 14)))\right\} P_{rated} \quad (5)$$

where DOY is the day of the year (1 to 365), h is the hour of the day and P_{out} will have the same units as P_{rated} (MW for a large power station). Using this approximation, when I_g decreases toward 0 Wm^{-2}, cell efficiency will drop to 65% of the ideal efficiency, comparable to the performance drop of a crystalline silicon PV cell [51]. During summer in the middle of the afternoon, P_{out} decreases further by up to 17% to account for heating related efficiency loss [51]. Both of these effects will decrease PR.

For rooftop PV systems, the tilt angle from horizontal was set to be 22.6° [52], and panels were assumed to be facing northward, although in reality there will be a spread of orientations around these values. The baseline installed capacity of rooftop PV arrays was taken to be 500 MW for the start of 2016, based on an installed capacity of 571 MW at 8th March 2016 [53].

There were more than 726,000 private dwellings in the greater Perth area in 2011 [54], of which under 10% are flats, units, apartments, or other types of dwelling that might be unsuitable for rooftop PV installation. The average floor area of houses in Australia is at least 150 m^2 [55]. Assuming that on average, a roof area equal to 25% of the floor area is suitable for north facing PV installation, then the total area per suitable house is 37.5 m^2. The current average size of a 250 W solar PV panel is 1.65 m^2, hence 22 panels could fit onto an average house, to give a maximum system size of 5.5 kW per house. If it was assumed that a 2% per year population growth rate translated into the same percentage growth in housing number, then the 653,403 suitable houses (90% of 726,004) in 2011 would grow into about 951,885 houses in 2030. Because of the spread of roof orientations, the simulation assumed a conservative total potential home rooftop capacity of 3.42 GW, consisting of 3.6 kW of north facing 22.6° tilt panels installed on 950,000 homes in 2030. Another factor that might affect the capacity is that the proportion of the population living in high density housing less suitable for rooftop PV will probably increase by 2030. Conversely, solar PV energy conversion efficiencies are also likely to increase by 2030.

For those scenarios with 100% renewable generation, the total PV capacity was de-loaded by 10% to enable frequency control capability. In reality, rooftop PV systems with battery storage would not need to operate in de-loaded mode (unless the battery storage level is low). If the batteries are installed behind the solar inverter, the inverter's output would still need to be limited to 90% of rated capacity for these systems, so

that the batteries can inject at least 10% (if storage level is adequate), but the PV panels can still operate up to full output when also charging the battery. Nevertheless, the total PV capacity was de-loaded, for model simplicity, and to avoid the assumption that all PV systems must be tied to a battery.

Solar thermal model

Solar thermal stations convert solar energy into thermal energy, which can be stored or passed into an electrical generation power block. In the areas of greatest solar resource within the SWWA, access to water could be a limiting factor, so it is preferable to use air-cooled generators, which have a lower water use requirement compared to water cooled generators. However air cooled generators have a lower efficiency. To offset this efficiency drop, solar thermal stations were modelled on power tower systems that use dual tracking heliostat mirror fields to focus sunlight onto a central tower receiver. These are considered able to achieve greater concentration of sunlight and higher temperatures than parabolic trough systems, which lead to higher efficiencies [56].

A generic energy balance model was used to estimate the energy flow through the solar thermal station. Unlike flat plate PV systems, concentrating solar power stations can only utilise the direct beam component of solar irradiance. Diffuse and reflected radiation are coming from many different directions, so they not be focused on the receiver by the mirrors. Thermal storage was modelled on a two tank molten salt system. Lower temperature molten salt is stored in the 'cold' tank, before being passed through the receiver where it is heated and then stored in the 'hot' tank. Some of this higher temperature molten salt is passed through the power block where a steam turbine system uses the heat to generate electricity. This cools the molten salt and it is passed back to the cold tank. The cycle can be repeated as long as there is enough sunlight hitting the receiver to reheat the salt.

The simulation attempts to maintain rated power output for as long as the combination of incoming solar radiation and heat storage allows. If the fraction of molten salt in the hot tank drops below a set operational minimum, then the thermal storage is considered to have been exhausted, and there will be no more electrical power output available from storage until the hot tank is replenished from solar radiation.

The model was calibrated to the power tower model used in the System Advisor Model (SAM)[57], such that the power output RMSE compared to SAM was less than 25%, and the stored energy RMSE was less than 10%. The overall solar to electric efficiency for a power tower with 15 hours storage was around 14.5%, slightly below the value of 15.8% predicted by Tyner and Wasyluk [58] for a power tower with 13 hours of storage, but close to the value of 14.6% modelled by Hinckley et al. [59] for a power tower with 6 hours of

storage using SAM. Hence the solar thermal model used in this study is slightly conservative. For a detailed description of the model, see Appendix A.

Wind power model

Wind is considered one of the cheapest forms of renewable energy, and renewable energy scenarios for Australia based on lowest cost have high penetrations of wind generation capacity [40]. To examine the potential for high levels of wind energy for the SWIS, a regional wind power model for the SWWA was developed, based on hourly wind speeds 50 m above the surface from the MERRA global atmospheric data base [60]. To scale these wind speeds to the hub height of the wind turbine, a spatially, diurnally and seasonally varying wind shear factor calculation algorithm was developed and calibrated to measured data. The wind power curves of individual turbines were modified and smoothed to represent the wind power output of whole wind farms consisting of these turbines. The correlation between the output of any two wind farms was also set to decrease as the distance between wind farms increased. The power output from this wind power model was compared to measured wind power generation from the six largest wind farms on the SWIS grid. The simulated values were found to have a similar distribution on hourly and daily time scales, but with conservative overall power output (Table 2). The average MBE between the yearly synthetic and measured values was -4.6%, and the average RMSE was 9.4%. For full details see Laslett et al. [42].

Table 2. Measured and simulated average yearly capacity factor (CF) for the six largest wind farms within the South West of Western Australia.

Name	Capacity (MW)	Measured CF	Simulation CF
Grasmere	13.8	0.33	0.32
Albany	21.6	0.32	0.32
Mumbida	55	0.39	0.38
Emu Downs	79.2	0.35	0.33
Walkaway	89.1	0.43	0.37
Collgar	206	0.37	0.33

A number of new wind farms in the SWWA have been proposed, with a total capacity of 1482 MW (Table 3). Since the wind power model was developed to cover the SWWA region, rather than one location, the hypothetical generation from these proposed wind farms could be estimated, as well as any other site chosen for a wind farm.

Table 3. Proposed wind farms in the SWWA region.

Name	Capacity (MW)
Dandaragan	513.4
Warradarge	250
Williams	210
Nilgen	132.5
Badgingarra	123
Coronation	104
Walkaway 2	94.05
Mileannup	55

Distributed energy storage model

Distributed energy storage for the simulation was loosely based on using batteries. Losses were incurred when energy is transferred from the grid to storage, and from storage to the grid. Additionally, limits were imposed on the maximum charging and discharging rates. For those scenarios with 100% renewable generation, the storage system was not allowed to become completely full or completely empty, so as to enable frequency stability control. For battery storage systems, the state of charge is often constrained between set limits to prolong battery life. In this study, storage capacity values refer to the capacity that is usable within these constraints rather than total capacity. The settings used are given in Table 4 below:

Table 4. Distributed storage simulation properties.

Maximum allowed storage level	95% of rated capacity
Minimum allowed storage level	5% of rated capacity
Grid-to-storage conversion efficiency	89%[a]
Storage-to-grid conversion efficiency	89%[a]
Maximum charge rate to storage	0.2 MW per MWh of storage[b]
Maximum discharge rate from storage	0.2 MW per MWh of storage[b]
Self discharge rate	3% per month[c]
Synthetic inertia	10 MWs per MWh of storage[d]

[a]Based on 90% round trip efficiency for Li-ion batteries [61] and 94% average PV inverter efficiency [49]. [b]McCloskey [62]. [c]Mishra et al. [63]. [d]0.2 MW/MWh x 50 MWs/MW [32].

Power-to-Gas (P2G) storage model

Since the SWWA region already has a natural gas supply network, methane was chosen as the gas storage medium. Estimates of the efficiency of the P2G process for methane range from 49% to 80% [64]. The overall

round trip efficiency (electricity to gas and back to electricity) depends on the efficiency of the gas turbine or other electrical generation technology. Weitemeyer et al. [16] used a round trip efficiency of 30%. This study assumed that a P2G plant would only operate when there was excess renewable electricity available, and so may operate at less than full capacity. The gas turbines were also assumed to operate at part capacity in response to changes in demand. Therefore the round trip efficiency was set at a lower value of 0.2 to account for efficiency losses due to these variable operating conditions. Since electricity was converted into methane only when excess generation was available, rather than at a constant rate, the total load demand was not increased. If charge level in the distributed energy storage system became low, then the P2G system was used to recharge the distributed storage, so that the overall combined generation capacity of both distributed storage and P2G could be maintained. The P2G storage methane leakage rate was set at 0.2% per month [65].

Energy efficiency model

Improving the energy efficiency of the devices that use electricity is a type of demand-side management, where the demand is permanently decreased, rather than increasing generation capacity. Modelling the improvement in instantaneous power consumption, throughout the day, for a single appliance, device or machine would be complex and dependent on individual usage patterns. However, the simulation assumed that in aggregate, these would level out, such that the saving in power demand through the day would be a constant fraction of the total load without efficiency improvements:

$$EE_h = \frac{eepc \times Load_{y,h}}{100} \tag{6}$$

where *eepc* is the percentage energy efficiency improvement.

Estimates of technically possible improvements in energy efficiency vary. Backlund et al. [66] estimated 25%, while Nadel et al. [67] estimated a median value of around 33%. Chua et. al. [68] estimated a 33% improvement in air conditioning efficiency was readily achievable (air conditioning is a significant portion of the summer peak load), and Matheisen et al. [38] assumed a 50% decrease in household electricity consumption was possible by 2050. However, there is also significant household use of gas, which is not counted as part of the SWIS electrical demand. Some energy efficiency improvements could result in a shift from gas use to electricity use, for example induction cook tops replacing gas cook tops and reverse cycle air conditioning replacing gas heating. Also other barriers may prevent full implementation, and the rebound effect, where efficiency improvements encourage greater use, may also reduce savings in energy use [69].

Therefore a middle range improvement value of *eepc* = 30% was used as a reference in this study, with 40% probably achievable. The current global average yearly reduction rate in energy intensity is around 1.5% [70]. If energy demand on the SWIS decreased at the same rate, then after 15 years the energy efficiency improvement would be about 20%, which was used as a lower bound.

3. Results

For the purpose of this study, the results of six scenarios were presented (Figures 3 to 7), although many more combinations are possible. The first scenario considered (S1) was a "small is beautiful" approach, where there is addition of more household solar and distributed storage capacity, and improvements in energy efficiency, but no more large power stations are added to the grid. Every suitable home was provided with a 3.6 kW rooftop PV and 12 kWh battery storage system. Assuming there were about 950,000 suitable houses available by the time installation was complete, the total capacity was 3.42 GW of rooftop PV with 11.4 GWh of storage. The PR of the roof top PV arrays was found to vary between 0.79 and 0.93, with the highest values occurring during winter. This was consistent with the findings of Carr and Pryor [50]. The modelling of this scenario indicated that although it was not possible to generate all of the power required by the SWIS using renewable energy, on many days the demand peak was substantially reduced, and shifted to later in the evening (for example Figure 8). The storage system also significantly reduced the maximum ramp rate required from dispatchable generation to balance supply and demand from over 20 MW per minute to under 8 MW per minute.

In this scenario, approximately 20 kWh per household per day on average was generated over a year. This is enough to supply the electricity use of every household on average, even without energy efficiency improvements, or moderate improvements counteracted by a shift from gas to electricity use.

To achieve 100% renewable energy generation, throughout the year, using only roof top PV arrays and storage required the addition of much more PV and storage capacity (Figure 9). This scenario (S2) required 19 GW of solar PV and 90.25 GWh of storage to achieve the SWIS reliability standards. This translates to about 20 kW of roof top PV and 95 kWh of storage per household. Winter was found to be the most challenging season to meet the energy demand due to the reduced availability of the solar resource and shorter day lengths. The storage requirement is at the upper end of the range of current electric vehicle battery capacities, but 20 kW of roof top PV per household is not currently feasible. However there is large untapped potential for commercial rooftop PV and the use of other surfaces. If a 250 W Solar PV panel has a surface area of 1.65 m^2, then 126 km^2 of solar PV arrays would be required, which is about 2.3% of the surface area of the Perth greater metropolitan area of 5386 km^2 [71].

A technical difficulty for this scenario is that the current SWIS grid is designed for power to flow unidirectionally from the transmission networks to the distribution networks. Residential households are connected to one of the distribution networks and may be supplied via roof top PV and home battery storage from other homes on the same network, but there may be imbalances in the supply and demand within each individual network. Also, some commercial or industrial loads may be connected to the higher voltage sub-transmission network and be inaccessible. Modification would be needed to enable bidirectional power flow between different distribution networks and the sub-transmission network.

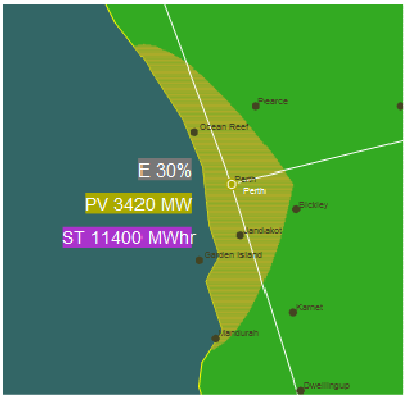

Figure 3. Scenario S1, "Small is beautiful": 3.42 GW Rooftop PV, 11.4 GWh of storage, 30% EE improvements. PV stands for photovoltaic, EE stands for Energy Efficiency.

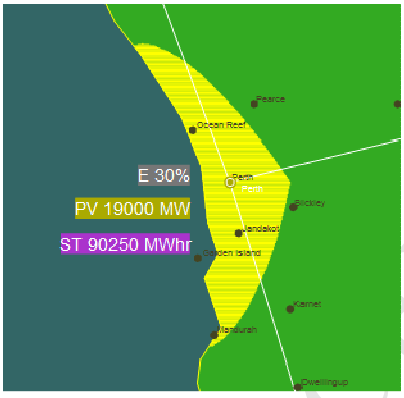

Figure 4. Scenario S2, "PV": 19 GW Rooftop PV, 90.25 GWh of storage, 30% EE improvements. PV stands for photovoltaic, EE stands for Energy Efficiency.

Figure 5. Scenario S3, "Solar thermal": 2.8 GW solar thermal (15h thermal storage), 6.84 GW Rooftop PV, 22.8 GWh of storage, 30% EE improvements. PV stands for photovoltaic, EE stands for Energy Efficiency.

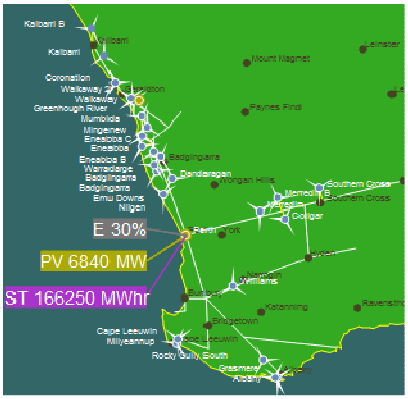

Figure 6. Scenario S4, "Wind": 7.947 GW wind, 6.84 GW Rooftop PV, 166.25 GWh of distributed storage, 30% EE improvements. PV stands for photovoltaic, EE stands for energy efficiency.

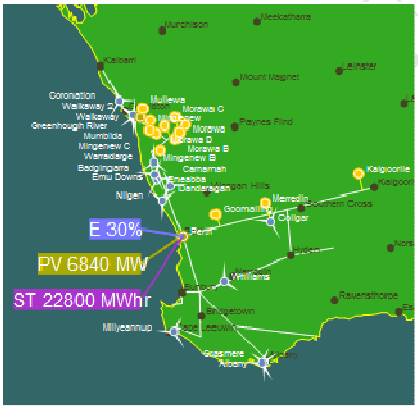

Figure 7. Scenario S5, "Mixed Solar thermal and wind": 2.5 GW solar thermal (15h thermal storage), 1.947 GW wind, 6.84 GW Rooftop PV, 22.8 GWh of storage, 30% EE improvements. PV stands for photovoltaic, EE stands for Energy Efficiency.

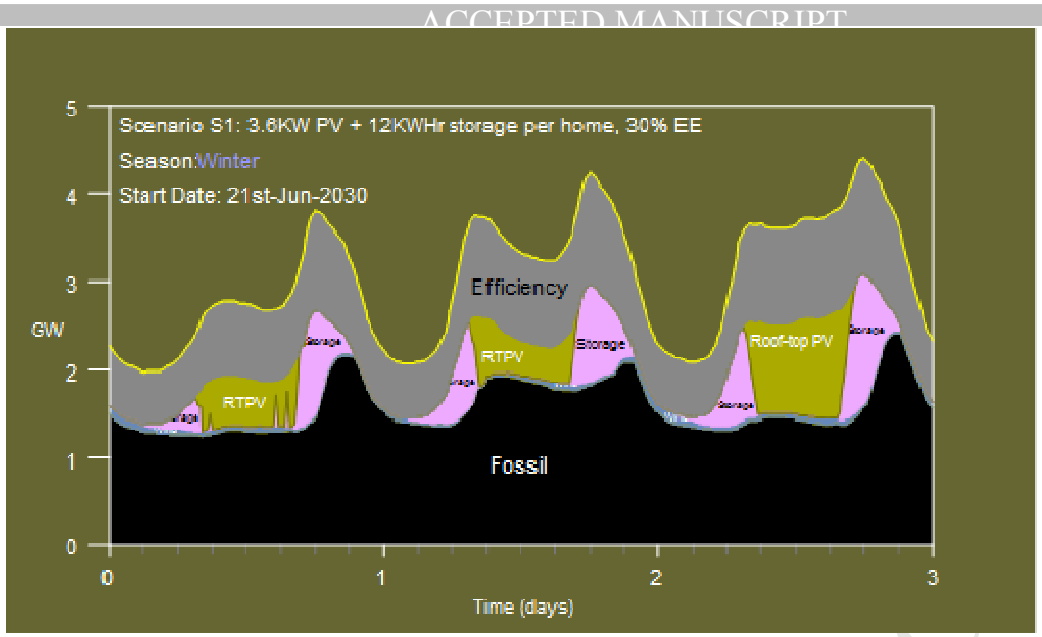

462

Figure 8. Example of winter demand peak reduction using household 3.6 kW rooftop solar systems with 12 kWh storage and 30% energy efficiency improvement (Scenario S1). Winter was chosen for this example for comparison with other scenarios. RTPV = Rooftop Photovoltaic arrays.

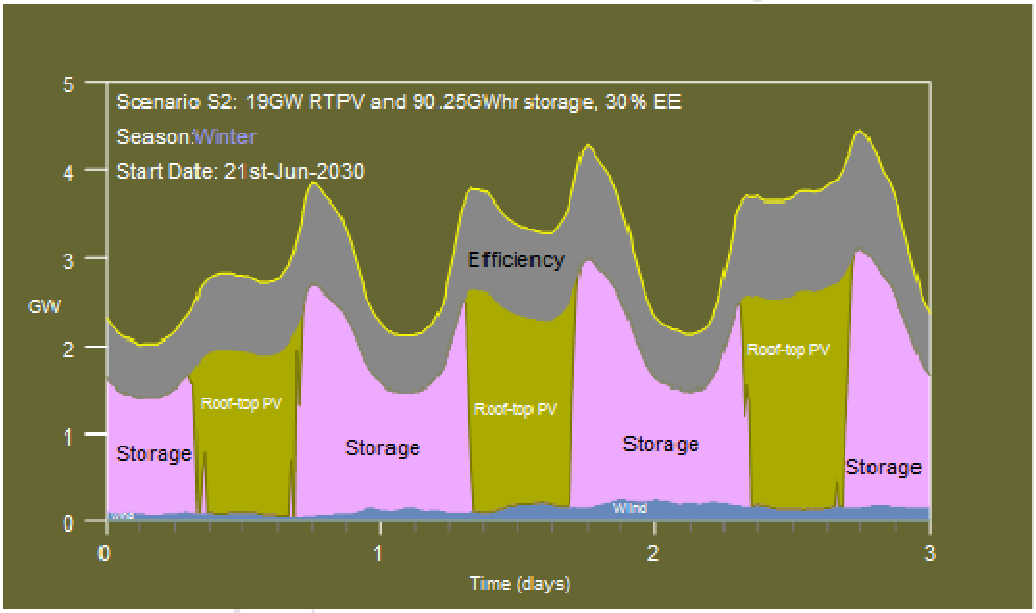

463

Figure 9. Example winter three day load profile of complete renewable energy generation using 19 GW of solar PV systems with 90.25 GWh of storage and 30% energy efficiency improvement (Scenario S2). Winter was chosen for this example because this season was found to be the most challenging to meet the energy demand due to the reduced availability of the solar resource and shorter day lengths.

464 An alternative (scenario S3) was to use solar thermal power stations with storage. In this scenario, overall
465 household capacity reaches 3.42 GW of PV and 11.4 GWh of storage, or 3.6 kW PV and 12 kWh per home as
466 before. The same again is added to commercial properties, to bring the total rooftop PV capacity to 6.84 GW

and storage capacity to 22.8 GWh. All further demand was met using a network of 14 solar thermal power stations, each with a capacity of 200 MW and molten salt thermal storage capacity of 15 hours. Four solar thermal stations were located to the east of Perth, to help stabilise the grid and take advantage of the solar resource in this low rainfall region. One of the stations was located fairly close to Perth to help provide high inertia centrally located generation, which provides a stable frequency reference for synchronous stability of remote generation. The largest cluster of solar thermal stations was located north of Perth to take advantage of the better solar resource at more northerly latitudes. For this scenario, winter was again found to be the most challenging season to meet the energy demand, and there was usually excess capacity over the summer months.

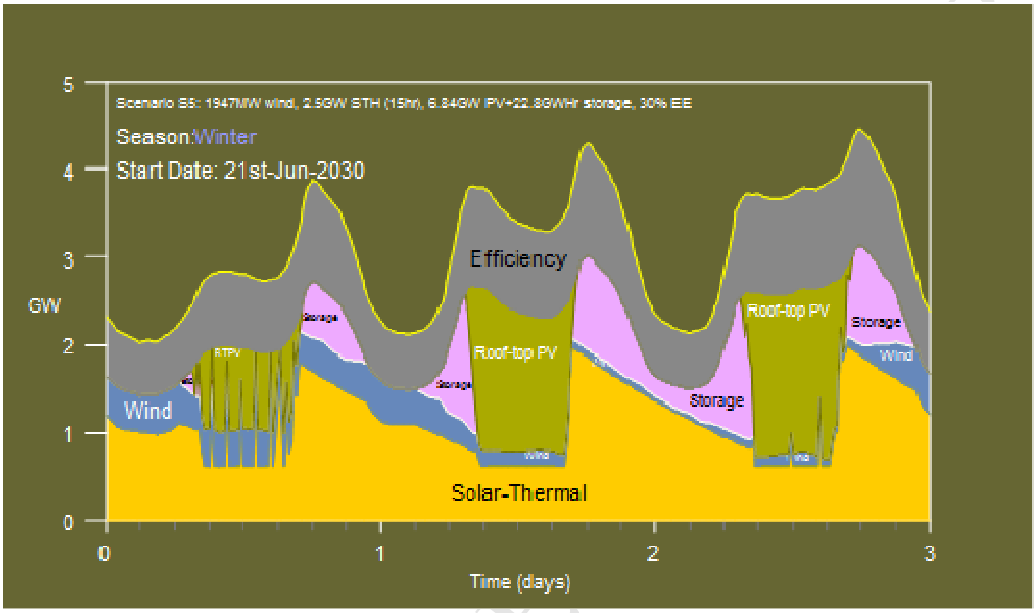

Figure 10. Example winter three day load profile of complete renewable energy generation using 2.5 GW of solar thermal stations (with 15h thermal storage), 1947 MW wind power, 6.84 GW rooftop solar PV systems with 22.8 GWh of storage and 30% energy efficiency improvement (Scenario S5). Winter was chosen for this example because this season was found to be the most challenging to meet the energy demand due to the reduced availability of the solar resource and shorter day lengths. RTPV = Rooftop Photovoltaic arrays.

A high wind power scenario was considered next. With 2% per year population increase and 30% energy efficiency improvements, the yearly average SWIS power demand by the year 2030 would be about 2.1 GW. Hence if the currently proposed wind farms were built the total wind power capacity would rise to 1947 MW, which could supply around 30% of grid electrical demand assuming the overall capacity factor remains between 0.3 and 0.45, similar to the existing wind farms (see Table 2). To meet the whole demand, it was found that increasing the wind power capacity to nearly 8 GW was required, along with enough storage capacity to balance the peaks and troughs in wind power output (scenario S4). Assuming that the total rooftop PV capacity reaches 6.84 GW as in scenario S3 before, it was found that a very large storage capacity of 166.25 GWh (6.93 gigawatt days) was needed to meet the SWIS reliability criteria 95% of the time over 100

simulation runs. This equates to 175 kWh of storage per home for 950,000 homes. If the storage capacity is the same as for scenario S3 above (22.8 GWh), then the energy supply shortfall was about 3%. However, the reliability standards could be met if a P2G plant capable of converting electricity to fuel at a rate of 450 MW was installed on the grid. In this scenario, about 80% of the energy generated was from wind.

Alternatively, if the currently proposed wind farms (1947 MW) were built along with solar thermal stations (scenario S5), then only 2.5 GW of solar thermal capacity needed to be built instead of 2.8 GW (Figure 10). If less distributed storage was installed, then the required solar thermal capacity increased (Figure 11).

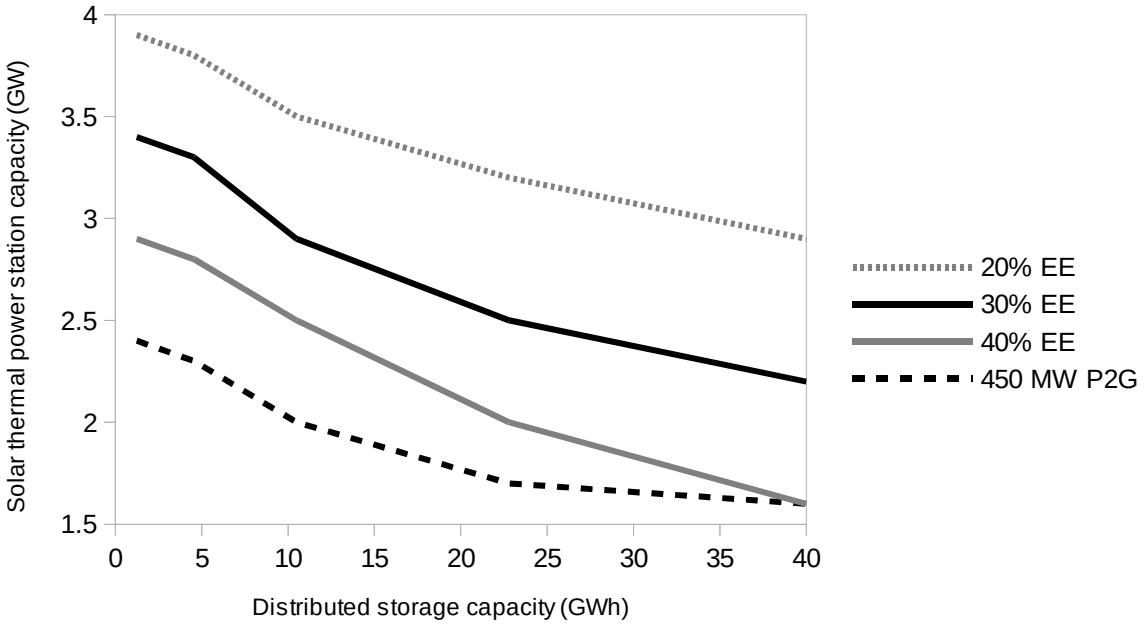

Figure 11. Solar thermal power plant capacity required for different levels of distributed storage capacity for variations of scenario S5. The input power capacity of the P2G system was 450 MW with round trip efficiency of 0.2. EE stands for energy efficiency improvement.

The sensitivity of the solar thermal capacity to the level of distributed storage reduced in magnitude as storage capacity decreased to very low levels or increased to very high levels. At low levels, storage was the constraining factor, and was provided by the thermal storage of the power plants. At high levels, storage had saturated and generation capacity was the constraining factor, also provided by the solar thermal power plants.

If a 450 MW P2G system was installed with round trip efficiency of 20%, similar to the high wind scenario S4, then required solar thermal capacity was decreased significantly at all storage levels (Figure 11), and to 1.7 GW at the reference 22.8 GWh distributed storage level. Alternatively, if no P2G system was used but energy efficiency measures were increased from 30% to 40%, then another 500 MW of solar thermal capacity

503 could be avoided at the reference 22.8 GWh storage level, reducing the total to 2 GW. At high storage levels
504 this 10% increase in efficiency was almost as effective as the P2G system at reducing the required solar
505 thermal capacity. However, if energy efficiency improvements only reached 20%, then the amount of
506 required solar thermal capacity increased by 700 MW at the reference 22.8 GWh distributed storage level.

507 The required capacities for each technology in each scenario were now finalised (Table 5), and the required
508 installation schedules for each scenario could be estimated (Table 6).

Table 5. Installed capacity for each 100% renewable scenario for the SWIS electrical grid.

Scenario	Energy efficiency	Solar PV	Distributed storage	Power to gas	Solar thermal	Wind
Current SWIS capacity	-	500 MW*	120 MWh*	-	-	465 MW
S2 PV	30%	19GW	90.25 GWh	-	-	465 MW
S3 Solar thermal	30%	6.84 GW	22.8 GWh	-	2.8 GW	465 MW
S4 Wind	30%	6.84 GW	166.25 GWh	-	-	7.947 GW
S4 + P2G	30%	6.84 GW	22.8 GWh	450 MW	-	7.947 GW
S5 Mixed solar thermal and wind	30%	6.84 GW	22.8 GWh	-	2.5 GW	1.947 GW
S5 + less EE	20%	6.84 GW	22.8 GWh	-	3.2 GW	1.947 GW
S5 + more EE	40%	6.84 GW	22.8 GWh	-	2 GW	1.947 GW

509 *Estimated

510 Solar PV, wind, and battery storage have exhibited the potential for exponential growth in installed capacity,
511 and energy efficiency improvements could be represented as a percentage reduction in energy demand.
512 When compared to current global growth rates (Table 7), the required growth rates for these technologies
513 were either less or similar in most cases, except for the high PV and wind scenarios S2, S4 and S4+P2G,
514 which would require accelerated roll out of distributed storage, and wind capacity for the high wind
515 scenarios. In all scenarios except the low efficiency scenario (S5 + less EE), to reach 30% energy efficiency
516 improvements in 15 years would require an accelerated reduction in demand compared to the current global
517 improvement rate. However the 2.35 to 3.35% rate of demand reduction per year seemed feasible, especially
518 since the amount of reduction actually decreases as demand reduces.

There is currently no installed capacity of solar thermal power tower and power to gas plants on the SWIS, so an exponential growth rate for these technologies could not be quantified. These are the least mature technologies. Required installed capacity for both was reduced by high installation rates of energy efficiency improvements and distributed storage.

Table 6. Yearly constant installation rates required for each 100% scenario to be completed by the year 2030.

Scenario	Energy Efficiency*	Solar PV	Distributed storage	Power to gas	Solar thermal	Wind
S2 PV	2%	1267 MW	6017 MWh	-	-	-
S3 Solar thermal	2%	187 MW	1520 MWh	-	187MW (or one 200MW plant per year for 14 years)	-
S4 Wind	2%	187 MW	11083 MWh	-	-	433 MW
S4 + P2G	2%	187 MW	1520 MWh	30 MW	-	433 MW
S5 Mixed solar thermal and wind	2%	187 MW	1520 MWh	-	167 MW (or one 200 MW plant per year for 12 years and then one 100 MW plant)	99 MW
S5 + less EE	1.33%	187 MW	1520 MWh	-	213 MW	99 MW
S5 + more EE	2.67%	187 MW	1520 MWh	-	133 MW (or one 200MW plant per year for 10 years)	99 MW

PV = Photovoltaic arrays, EE = Energy efficiency improvement. *% reduction of load demand with no efficiency improvements.

For all of the 100% renewable energy scenarios (S2 to S5), it was found that winter was the most challenging time for the power systems, because of the lower availability of solar and wind resources, and shorter day length. Therefore significant extra capacity had to be installed, resulting in generation overcapacity during the summer months. For all of these scenarios, the reference storage capacity was 22.8 GWh. Reserving the upper and lower 5% of storage capacity to provide synthetic inertia meant that the storage system could provide at least 228 GWs of inertia, much greater than the 12.4 GWs of inertia on the present SWIS grid

(Table 8), and also absorb or supply more than 4 GW of power for 15 minutes in response to a sudden load change or generation fault. 15 minutes is enough time for the spinning reserve generators to start generating power and provide spinning reserve if required. Hence this storage system could provide frequency stability control services as well. To provide these services a portion of the storage capacity would have to be connected directly to the transmission and sub-transmission networks, rather than the distribution networks that connect most homes. The lowest storage level considered in Figure 11 was 1.24 GWh, enough to provide the same inertia as the present SWIS grid.

Table 7. Yearly exponential installation rates for each 100% scenario to be completed by the year 2030.

Scenario	Energy efficiency	Solar PV	Battery storage	Wind
Current SWIS capacity	-	500 MW*	120 MWh*	465 MW
Global growth rate 2015	1.5%[a]	28%[b]	50%[c]	17%[b]
S2 PV	2.35%	27.5%	55.5%	-
S3 Solar thermal	2.35%	19%	41.9%	-
S4 Wind	2.35%	19%	62%	20.8%
S4 + P2G	2.35%	19%	41.9%	20.8%
S5 Mixed solar thermal and wind	2.35%	19%	41.9%	10%
S5 + less EE	1.48%	19%	41.9%	10%
S5 + more EE	3.35%	19%	41.9%	10%

*Estimate. [a]% reduction in energy intensity per year [70]. [b][70]. [c] [72].

Table 8. Synthetic inertia from reserving the upper and lower 5% of storage capacity for each 100% renewable energy scenario.

Scenario	Storage (GWh)	Inertia (GWs)	Current SWIS inertia (GWs)
S2	90.25	902.5	12.4
S3	22.8	228	12.4
S4	166.25	1662.5	12.4
S4 + P2G	22.8	228	12.4
S5	22.8	228	12.4
S5 + less EE	22.8	228	12.4
S5 + more EE	22.8	228	12.4

For scenarios S3 to S5, most of the large generators are far from the main load centre (the Perth area). Therefore the spinning synchronous compensator reserve close to Perth may aid the synchronous stability of the large remote generators.

4. Discussion and Conclusions

The results of this simulation indicated that for typical weather conditions it is feasible to supply 100% of the electrical demand of the SWIS system, projected out to the year 2030, on an hour by hour basis using a combination of energy efficiency measures, residential and commercial roof top photovoltaic systems, solar thermal power stations with heat storage, wind power and distributed battery storage systems. All of these technologies are currently available, with energy efficiency, wind, solar PV, in large scale commercial operation and battery storage approaching large scale production.

The use of battery storage enabled buffering of the variable output of solar PV and wind farms. Thus the maximum ramping rates required of the dispatchable generators could be limited. This has the potential to reduce costs during transition periods when both renewable power generators and conventional fossil based generators are connected to the grid. The reference level of storage in the 100% renewable energy scenarios (S2 to S5) meant that, as well as providing synthetic inertia, participation in primary and secondary frequency stability control services was possible. This would reduce the need to keep existing synchronous generators spinning to provide these services, however they are needed to provide a backup in the case of generation shortfall or transmission line fault. The estimated synthetic inertia for these scenarios (S2 to S5) was greater than the inertia currently on the SWIS grid, confirming that the amount of distributed battery storage is compatible with grid stability.

The simulation assumed typical weather conditions in which the solar and wind resources are strongest in the summer season and weakest in the winter season, when day length is short. Similar to the findings of Elliston et al. [10], the winter evening peak period was the most difficult to supply, and there was usually large overcapacity in the summer months. If winter weather conditions are encountered that cause a shortfall in generation from solar and wind, then a reserve source of energy could be used to maintain storage levels and required generation.

The results of this study indicated that a power to gas system could act as a reserve and significantly reduce either the required solar thermal and storage capacity, or both, and may be necessary for a high wind power scenario to meet SWIS reliability standards without a very large amount of storage. However this technology is still in the development stage. The balance between using more distributed storage or more P2G capacity

would be an economic decision as well as a technical one. Improving the flexibility and efficiency of P2G systems should be a priority. Improving energy efficiency reduced the capacity of solar thermal power, distributed storage or P2G needed to supply the demand.

Alternatively to P2G, a renewable energy resource that is strong during the winter months, such as wave power [73], could be utilised. Wave power technology is advancing into commercial operation and it is worthwhile modelling the potential contribution to the SWIS grid. Another possible option is the use of biomass, which can be stored on seasonal time scales until it is needed, but attracts controversy over the use of native forest wood for fuel and the substitution of food production for energy production. Oil mallee biomass [74], from land in the wheat belt that cannot be used for food, may avoid both problems. However the capacity for sustainable large-scale production must be modelled, and also biomass cannot utilise any excess summer electrical generation from solar and wind. There have been proposals for ocean water pumped hydro storage systems that utilise the height of coastal cliffs [75], as an alternative to battery storage. These could also store excess energy on seasonal time scales, and could utilise excess summer generation, although the main use is likely to be on daily time scales.

The installation rates required to implement each of the scenarios differed significantly, particularly with the yearly addition of storage capacity required. The predominant wind scenario S4 required the highest uptake at almost 11.1 GWh per year, or almost 64,000 homes per year with 175 kWh of storage each, which seems unrealistic. However if a more realistic storage level was reached, and there was some other form of renewable energy available to cover the shortfall, then this scenario might be more viable, and is worth investigation as wind power is one of the lowest cost forms of renewable energy. The mixed solar thermal and wind scenario S5 had the most balanced uptake rate, with reduced uptake rates for solar thermal power stations compared to the predominant solar thermal scenario S3. Solar thermal power station technology is perhaps the least commercially mature but the requirement to build one 200 MW plant per year seems feasible. Wind power is the most commercially mature technology, however uptake rates are limited by transmission line capacity limitations and necessary approval processes even though much of the land used by wind farms can still be used for other purposes. Use of the currently proposed new wind farm projects could be expected to reduce the lead times required. Energy efficiency, roof top PV, and distributed storage can perhaps be implemented the fastest, as they require no or little extra land. The value of implementing energy efficiency measures in reducing the required generation was demonstrated in scenario S5 and should be considered one of the most effective components of a large scale renewable energy electricity system. However, further improvements in energy efficiency become more difficult as efficiency improves.

The development of this interactive web browser based simulation tool allowed different scenarios to be easily considered and modified, and allowed easy accessibility. It was possible to examine renewable energy

scenarios for large regional electricity networks without high computing power, although running 100 one year simulations took several minutes to complete. Although grid stability at sub hourly time scales was not explicitly modelled, which would require more computing power, it was taken into account. However this tool cannot be used to decide precise locations for renewable energy power stations, as the solar and wind models are designed for simplicity and quick computation. Instead an idea of the scale of renewable energy capacity required can be gained. Much more detailed solar and wind resource modelling, land use mapping and transmission system planning would be required to decide the actual sites. The purpose of this tool was flexible scenario building.

This study modelled a snapshot of the possible SWIS hourly demand profile in the year 2030. Faster population increase, large-scale adoption of electric vehicles or a large-scale switch from using gas to using electricity could all significantly increase the demand for electricity from the SWIS grid, and hence the need to build more renewable energy capacity and improve energy efficiency. Improvements in energy efficiency could compensate for population growth in the short to medium term. Reductions in transportation energy use would require significant uptake of public transport and reorganisation of economic activity. The rooftop area available for PV could be affected by changes in the housing mix as population grows. Conversely, improvements in PV cell efficiency will increase the capacity available for a given rooftop area. The urgency of reducing emissions is balanced by renewable energy technologies that are expanding rapidly on a global scale, which makes the task realistic. This study demonstrated the feasibility of a rapid build 100% renewable energy system for the SWIS electrical grid.

If the target was delayed until 2050, more capacity may be required to meet increased demand (assuming population growth continues at the same rate), but there is also more time to gain further energy efficiency improvements, solar PV cell efficiencies are likely to increase further, perhaps wind turbine capacity factors will be greater, and there is more time to build the required capacity, so the build schedule would be more relaxed than the 2030 target. The cost of many of the technologies discussed here are falling, so they may be even cheaper by 2050. A fully renewable energy system may be built well before 2050 for purely financial reasons. An unknown factor would be that climate change may have affected the wind patterns across the SWWA to a greater extent and also the solar radiation patterns. Although an electrical system based more on distributed generation and storage could be expected to be more resilient, aiming for a 2030 target to avoid the increased risk of disruptive extreme weather events from dangerous climate change is preferable.

Acknowledgements

Thanks to Murdoch University for supporting my candidature, and the National Aeronautics and Space Administration (NASA) for providing open access to the MERRA database.

Appendix A. Detailed solar thermal station model

The type of solar thermal technology modelled was a central tower receiver system surrounded by a field of dual-axis tracking heliostat collectors. The central tower was linked to a thermal to electrical generation power block via a two tank molten salt thermal storage system. For each solar thermal station in a scenario, the following algorithm was used to calculate the power output and energy stored. At a particular hour of the day, the available solar radiation power input, P_{in} (MW), to be converted into heat and then electrical output power was calculated using:

$$P_{\text{in}} = 10^{-6} I_{bn} ca \tag{A1}$$

where I_{bn} is the beam irradiance falling normal to the collector array (W/m^2), and ca is the collector surface area (m^2). I_{bn} is obtained from the solar radiation model [41]. The required collector area is dependent on the rated power. Firstly, a reference, or 'design point', base collector area, car (m^2), was calculated by assuming that the rated output power, P_{rated} (MW), would be achieved if the sun was at the solar zenith position (directly overhead), and a reference beam normal solar irradiance I_{bnref} (often around 1000 W/m^2) was falling on the whole collector array:

$$car = 10^{6} \frac{P_{rated}}{I_{bnref} e_{st} e_{te}} \tag{A2}$$

where e_{st} is the design point solar-to-thermal conversion efficiency, and e_{te} is the design point thermal-to-electrical conversion efficiency. e_{te} includes parasitic electrical power required to keep the plant operating. It can be expected that some of the collectors in the array are off line at any one time for troubleshooting or routine maintenance. In the simulation, this is assumed to be a constant percentage of the total collector area. The online fraction olf can be defined as:

657

$$olf = 1 - \frac{capcdown}{100} \quad \text{(A3)}$$

658

659 where *capcdown* is the average percentage of the collector array that is off line at any one time. If the solar
660 thermal station has no storage, then the collector area required to deliver the rated power to the load at the
661 reference beam solar irradiance was calculated as:

662

$$can = \frac{car}{olf} \quad \text{(A4)}$$

663

664 where *can* is the no-storage collector area (m^2). For solar thermal stations with thermal storage, the collectors
665 must provide for the energy to be stored as well as that immediately transformed into electricity, thus the
666 collector surface area will be greater and is dependent on the rated design storage time, t_s (hours). For the
667 storage medium, the maximum energy stored per unit volume E_{sv} (J/m^3) over the rated storage time t_s hours
668 was calculated using:

669

$$E_{sv} = C_v(temp_{hot} - temp_{cold})(1 - 0.01 r_{leak} t_s) \quad \text{(A5)}$$

670

671 where C_v is the storage medium volumetric heat capacity ($J\ m^{-3}°C^{-1}$), $temp_{hot}$ is the operating temperature of
672 the storage medium (°C) after heating, $temp_{cold}$(°C) is the operating temperature of the storage medium after
673 cooling to produce electricity, and r_{leak} is a heat leakage loss term (% per h). The storage energy E_{ts} (J) required
674 to maintain the rated output power over the rated design storage time was calculated using:

675

$$E_{ts} = 3.6 x 10^9 P_{rated} \frac{t_s}{e_{te}} \quad \text{(A6)}$$

676

677 Therefore the effective required storage medium volume *svi* (m^3) can be calculated as the ratio of E_{ts} and E_{sv}:

678

$$svi = \frac{3.6\,x\,10^{9} P_{rated}\, t_s}{e_{te} C_v (temp_{hot} - temp_{cold})(1 - 0.01\, r_{leak}\, t_s)} \quad \text{(A7)}$$

679

680 The final storage volume *sv* (m^3) was calculated assuming *svi* must be overrated to compensate for
681 troubleshooting and maintenance downtime:

682

$$sv = \frac{svi}{olf} \quad \text{(A8)}$$

683

684 Since not all of the storage medium will always be at the heated temperature $temp_{hot}$, the leakage loss rate will
685 be less than $loss_{max}$. Hence the storage medium volume has also been overrated to compensate for any
686 foreseeable thermal losses.

687 The total required collector area for operation and storage was calculated using the effective operational
688 storage volume *svi*. To be able to load the storage medium with enough energy to provide the rated power
689 for the rated storage time:

690

$$10^{6}\, cas\, TDR\, e_{st}\, olf = 3.6\,x\,10^{9} \frac{P_{rated}\, t_s}{e_{te}} + 0.01\, r_{leak}\, t_s C_v (temp_{hot} - temp_{cold})\, svi \quad \text{(A9)}$$

691

692 where *cas* is the extra collector area required for storage (m^2), and *TDR* is the total daily radiation ($MJ/m^2/d$),
693 which will depend on the location, season, and the local weather. Combining with equation A7 and
694 rearranging gives:

695

$$cas = \frac{3600\, t_s\, P_{rated}}{TDR\, e_{st}\, e_{te}\, olf} \left(1 + \frac{0.01\, r_{leak}\, t_s}{1 - 0.01\, r_{leak}\, t_s}\right) \quad \text{(A10)}$$

696

697 The solar multiple, *sm*, can be defined as the ratio of total required collector area to collector area without
698 storage:

699

$$sm = \frac{can + cas}{can} \quad \text{(A11)}$$

700

701 or

702

$$sm = 1 + \frac{3.6\, I_{bnref}\, t_s}{1000\, TDR} \left\{ 1 + \frac{0.01\, r_{leak}\, t_s}{1 - 0.01\, r_{leak}\, t_s} \right\} \quad \text{(A12)}$$

703

704 At high values of solar multiple, large single unit power towers can run into limitations on tower height,
705 receiver size and heliostat distance from the central receiver [76], hence *sm* was limited to a maximum value
706 of 3.5. The total collector area *ca* (m^2) was calculated using:

707

$$ca = can \times sm \quad \text{(A13)}$$

708

709 The total effective collector area cae (m^2) is:

710

$$cae = olf \times ca \quad \text{(A14)}$$

711

712 Choice of the value of TDR depends on how the solar thermal plant will be used. If a lower TDR from a
713 typical winter day is chosen, then the solar multiple will be higher and the plant is more likely to be able to
714 maintain output during the winter months. However the required heliostat field area and construction costs
715 will be greater, and there will more likely be excess irradiance during the summer months, forcing some of
716 the heliostats to move focus away from the receiver. Conversely a higher TDR will decrease the solar
717 multiple but increase the likelihood of the plant not being able to heat all of the storage medium on a day of
718 low TDR.

719 The design point solar to storage conversion efficiency e_{st} was divided into two components, the design point
720 heliostat solar field efficiency e_{sr} (or the solar-to-receiver efficiency) and the design point receiver-to-storage
721 efficiency e_{rt}:

722

$$e_{st} = e_{sr}\, e_{rt} \quad \text{(A15)}$$

723

Singer et al. [77] and Gauche et al. [78] found that the heliostat solar field efficiency drops off from its design-point value at low solar altitude angles. The solar altitude angle α measures the vertical angular distance between the sun and the horizon. A heuristic equation was developed to approximate this effect (see also Fig. 12):

$$P_{recin} = P_{in} e_{sf} \left\{ 0.2 + \sin\alpha \left(0.2 + \frac{7.8}{1 + 12\sin\alpha} \right) \right\} \quad \text{(A16)}$$

where P_{recin} is the input power from the solar field to the central receiver (MW).

Figure 12

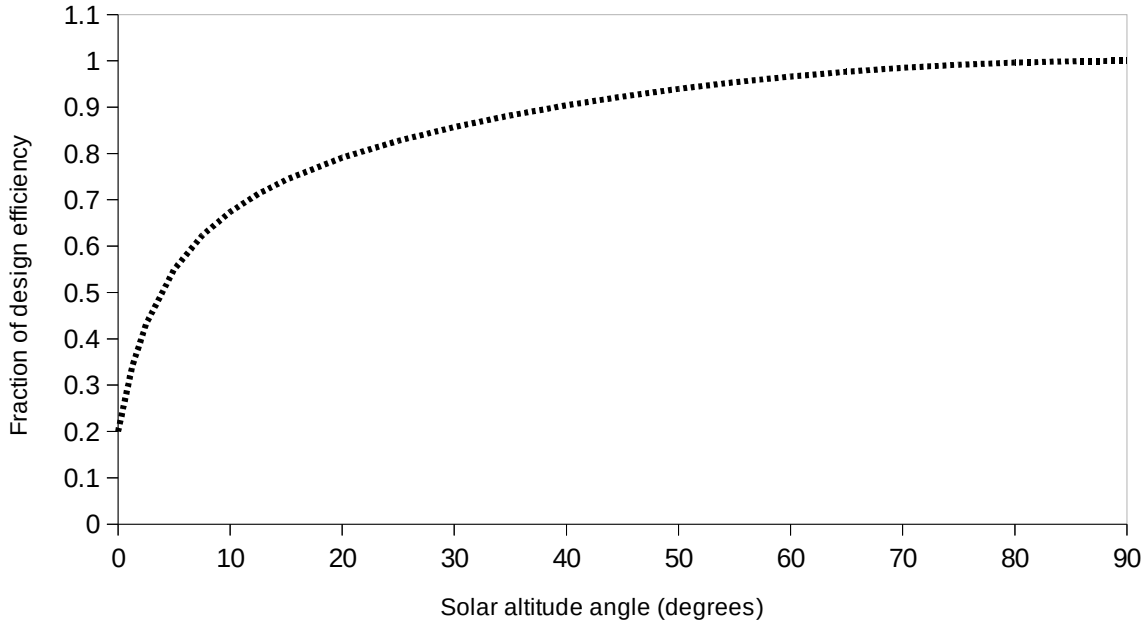

. Approximation of solar to receiver efficiency drop off with low solar altitude angle.There is also an efficiency drop when the solar power incident on the central receiver, P_{recin}(MW), is much less than the design-point receiver input power P_{recr} (MW), or more than P_{recr}. A heuristic equation was developed to approximate this effect (see also Fig. 13):

There is also an efficiency drop when the solar power incident on the central receiver, P_{recin}(MW), is much less than the design-point receiver input power P_{recr} (MW), or more than P_{recr}. A heuristic equation was developed to approximate this effect (see also Fig. 13):

$$P_{storein} = P_{recin} e_{rt} \left\{ 0.775 + 0.45 \frac{(P_{recin}/P_{recr})}{1+(P_{recin}/P_{recr})^3} \right\} \quad \text{(A17)}$$

where $P_{storein}$ is the power input to the thermal storage medium (MW). The receiver was designed so that P_{recr} is a multiple of the thermal power needed by the power block to generate P_{rated} MW of electrical power:

$$P_{recr} = \frac{P_{rated} sm}{e_{te}} \quad \text{(A18)}$$

If there is thermal storage, *sm* should be greater than 1 so that the receiver has enough capacity to transfer energy to the storage medium as well as the power block. The model also assumed that P_{recin} did not exceed a maximum limit P_{recmax}, which is slightly larger than P_{recr}. Some heliostats would be focused away from the receiver if there was excess solar power input.

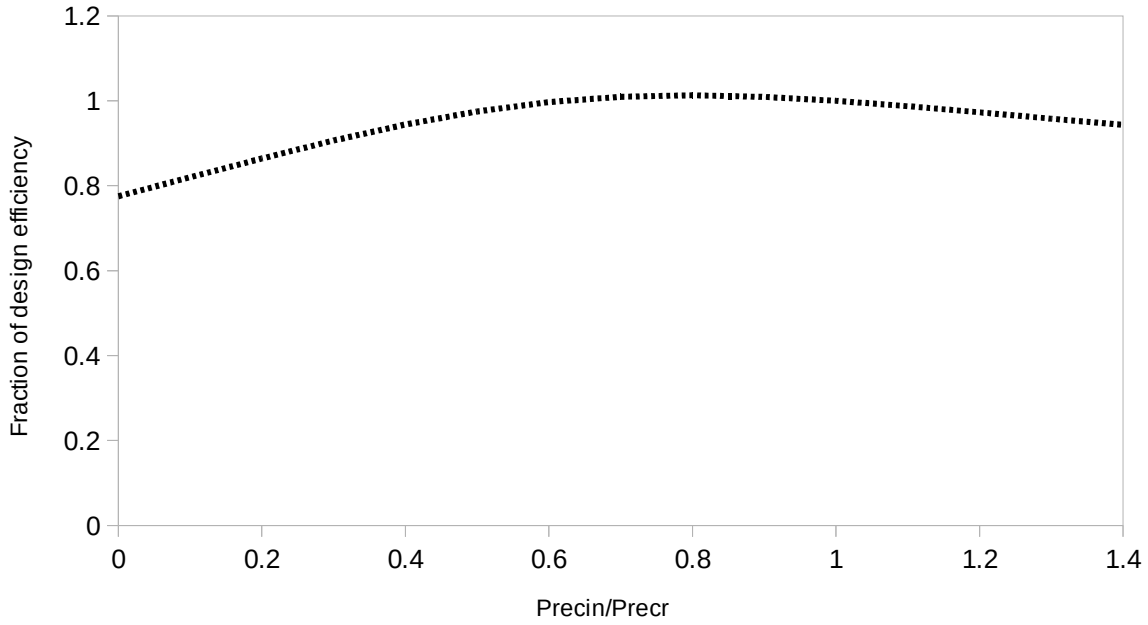

Figure 13. Receiver to storage efficiency drop off with low receiver input power.

Let P_{req} be the power output requested by the grid (MW). P_{req} can range from zero to P_{rated}. Let P_{out} be the actual power output of the power plant (MW). P_{out} can range from zero to P_{req}. The design point storage-to electrical-efficiency was divided into design point storage to thermal efficiency e_{tpb}, power block thermal-to-electrical efficiency e_{pb} and parasitic losses:

749

$$e_{te} = e_{tpb} e_{pb} (1 - 0.01 r_{parasitic}) \quad \text{(A19)}$$

750

751 where $r_{parasitic}$ is the plant electrical parasitic loss factor (%). Wagner and Zhu [79] approximated power block
752 efficiency decreases under part load conditions (Figure 14) with:

753

$$P_{out} = e_{te} P_{storeout} \left(0.5628 + 0.8685 f_{out} - 0.5164 f_{out}^2 + 0.0844 f_{out}^3\right) \quad \text{(A20)}$$

754

755 where $P_{storeout}$ is the power output from the thermal storage medium (MW) and $f_{out} = P_{out}/P_{rated}$. If $P_{storein} > P_{storeout}$,
756 then energy is transferred to storage. Conversely, if $P_{storein} < P_{storeout}$, then energy is transferred from storage. As
757 long as there is enough energy stored in the heated thermal storage medium, output power P_{out} is P_{req}. The
758 change in heated fraction of the storage medium, Δf_{hot}, for one time step of the simulation was estimated
759 using:

760

$$\Delta f_{hot} = \frac{3.6 x 10^9 t_{step} (P_{storein} - P_{storeout})}{C_v \, svi \, (temp_{hot} - temp_{cold})} - 0.01 r_{leak} t_{step} \quad \text{(A21)}$$

761

762 where t_{step} is the time step (h). If f_{hot} reaches 1, then it was assumed that the power plant control system would
763 allow no further increase by defocusing some or all of the heliostat collectors. If f_{hot} falls below a threshold
764 $f_{hot,shutdown}$, the power plant goes to stand by, then shuts down if there is no more incident solar power from the
765 heliostats hitting the receiver. Output from the power plant is reduced to zero. If this occurs during night
766 time, then I_{bn} will remain at zero until the next dawn and the power station will produce no power until
767 then.

768 For the power station to restart, first the heliostats must focus, then the receiver must restart, and then the
769 power block must restart. The heliostats were set to focus on the receiver after dawn when the solar altitude
770 angle rose above the deploy angle α_{deploy}. They were also set to defocus and stow before dusk when the solar
771 altitude angle dropped below α_{deploy}. The receiver was set to restart once incident solar power from the
772 heliostats reached a minimum fraction $f_{rstartup}$ of receiver rated power P_{recr}. The power block was set to restart
773 once the receiver was fully operational. Both receiver and power block start ups were modelled as two stage

774 processes (Tables A9 and A10). The receiver was shut down if the incident solar power dropped below $f_{rstartup}$,
775 which happens immediately after the heliostats stow, before dusk.

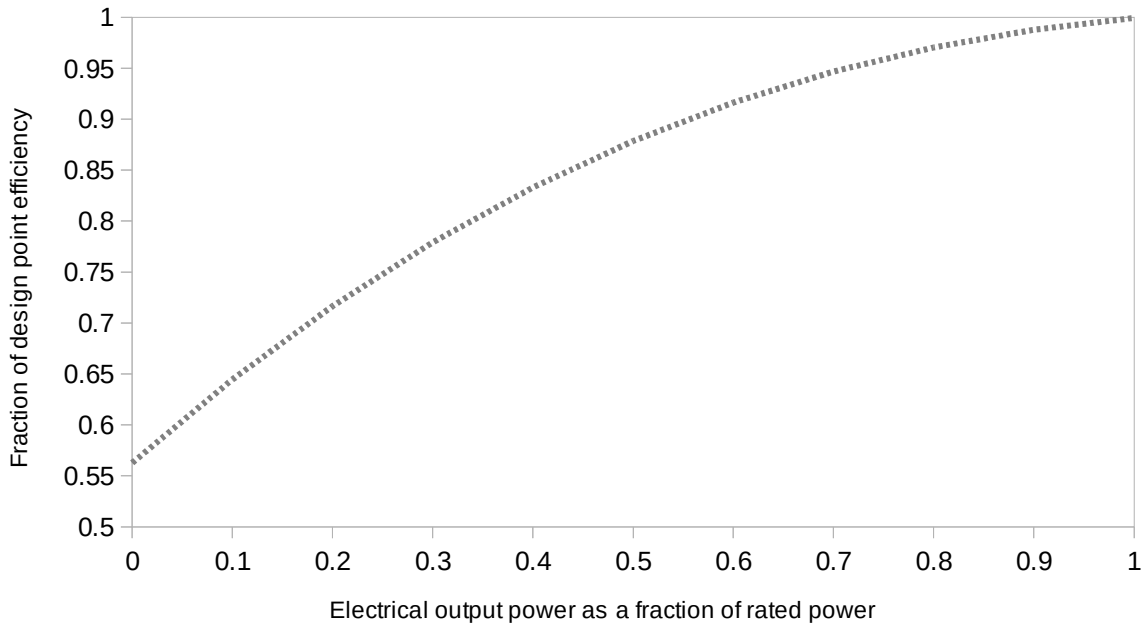

776

Figure 14. Storage to electrical efficiency drop off with low electrical output power.

Table A9. Start up stages for the solar thermal power tower receiver.

stage	name	time period (h)	description
0	shut down	-	The receiver is shut down. No thermal energy is transferred to storage.
1	start up	0.2	The receiver is warming up. No thermal energy is transferred to storage.
2	operating	-	Normal operation. Thermal energy transferred to storage

Table A10. Stages for the solar thermal power tower power block.

stage	name	time period (h)	description
0	shut down	-	Plant generates no electrical power
1	start up	0.5	Heat transferred from storage to power block. No power generated. After time period is up, go to stage 3
2	stand by	0.5	Heat transferred from storage medium to power block. No power generated. If more solar power is being transferred to receiver, then go back to stage 3 (operating). Otherwise, after time period is up, go to stage 0 (shut down).
3	operating	-	Normal operation.

777

A maximum ramp rate condition and minimum operational power level was also placed on the output power P_{out}:

$$-maxramp < \frac{P_{out}(t) - P_{out}(t - t_{step})}{60 t_{step}} < maxramp \quad \text{(A22)}$$

$$P_{out} \geq f_{outmin} P_{rated} \quad \text{(A23)}$$

where *maxramp* is the maximum allowable ramping rate of the electrical output power (MW/min), and f_{outmin} is the minimum operating level as a fraction of rated output power P_{rated}. If the requested power P_{req} is lower than the minimum operating level, then P_{out} can be lowered, but the thermal power required by the power block will remain at the same level as if $P_{out} = f_{outmin} P_{rated}$.

The design-point operating temperature ranges and physical quantities used for the simulation are given in table A11 below.

Table A11. Solar thermal station operating constants.

Constant	Description	Value
I_{bnref}	reference beam normal solar irradiance	986 W/m^2[a]
TDR	total daily radiation used to calculate solar multiple	18 MJ/m^2/d[b]
e_{sr}	solar field efficiency at design point	57.5%[c]
e_{rs}	receiver-to-storage efficiency at design point	92.7%[c]
e_{tpb}	storage to power block efficiency	99%[c]
e_{pb}	power block thermal to electrical efficiency at design point	41.2%[c]
$r_{parasitic}$	electrical parasitic losses	10%[d]
capcdown	average off line percentage of collector array and storage	10%[e]
$temp_{cold}$	cooled storage medium temperature	290 °C[e]
$temp_{hot}$	heated storage medium temperature	565 °C[e]
r_{leak}	thermal storage medium heat leakage rate	0.031% per hour[f]
$f_{hot,shutdown}$	threshold heated fraction of thermal storage medium for shut down	0.05/storage time in hours[aa]
C_v	volumetric heat capacity	2.785 MJ/m^3/°C[g]
f_{outmin}	minimum operational electrical output as a fraction of P_{rated}	0.25[c]
α_{deploy}	solar altitude angle at which heliostats deploy and stow	8°[c]
$f_{rstartup}$	minimum receiver incident power as a fraction of receiver rated power	0.25[c]

maxramp	maximum ramp rate	6% of rated capacity/min[h]

789 [a]Spencer [80]. [b]Gives solar capacity factor ~0.21. [c]Calibration with System Advisor Model [57].[d]Avila et al. [81]. [e]Singer et al. [77].

790 [f]Madaeni et al. [82]. [g]Bayon and Rojas [83]. [h]Denholm et al. [84].

Appendix B. Nomenclature

α_{deploy}	solar altitude angle at which heliostats deploy and stow
Δf_{hot}	change in solar thermal storage heated fraction for one time step (°C)
ca	collector area (m^2)
cae	total effective collector area (m^2)
can	no-storage collector area (m^2)
capcdown	average off line percentage of solar thermal collector array and storage
car	reference collector area (m^2)
cas	collector area required for storage (m^2)
C_v	storage medium volumetric heat capacity (joules $m^{-3}°C^{-1}$)
d_j	length of grid link j (km)
EE_h	load demand reduction at hour h due to any energy efficiency measures if implemented (MW)
e_{pb}	power block thermal to electrical efficiency at design point
e_{rs}	receiver-to-storage efficiency at design point
e_{sr}	solar field efficiency at design point
e_{st}	solar thermal solar-to-storage efficiency
E_{sv}	maximum energy stored per unit volume (joules/m^3)
e_{te}	solar thermal storage-to-electrical efficiency
e_{tpb}	storage to power block efficiency
E_{ts}	storage energy required to maintain rated output power over rated design storage time (joules)
f_{hot}	fraction of storage medium heated to $temp_{hot}$
$f_{hot,shutdown}$	threshold heated fraction of thermal storage medium for shut down
f_{out}	solar thermal power station electrical output as a fraction of P_{rated}
f_{outmin}	minimum operational electrical output as a fraction of P_{rated}
$f_{rstartup}$	minimum receiver incident power as a fraction of receiver rated power
glf	grid power loss factor between power plant and load centre (Perth), or in the case of rooftop PV, the distribution loss factor
HVAC	High Voltage Alternating Current
I_{bn}	beam normal solar irradiance (W/m^2)
I_{bnref}	reference solar beam normal irradiance
I_g	global solar irradiance (W/m^2)
ld	grid step-down and distribution loss (%)
$Load_{y,h}$	SWIS load demand for year y at hour h (MW)
LOLP	loss of load probability
lossfact	thermal storage loss factor (sec^{-1})
$loss_{max}$	maximum loss factor (W/m^3)
lup	grid up-conversion and cross-conversion loss (%)
maxramp	maximum solar thermal station ramp rate (% rated capacity/min)
MBE	mean bias error
n_{large}	number of large-scale renewable power stations

nlink	number of grid links travelled by power between power station and load centre (Perth)
nonre	non-renewable power generation (MW)
olf	online fraction
P_{in}	available power input from sun (W)
pop	percentage yearly population increase (% per year)
P_{out}	power plant actual output power (MW)
PR	performance ratio
P_{rated}	power plant rated output power (MW)
P_{recin}	solar power incident on the central receiver (MW)
P_{recr}	design-point receiver input power (MW)
P_{recmax}	maximum receiver input power (MW)
P_{req}	power plant output power requested by the grid (MW)
$P_{storein}$	power input to thermal storage
$P_{storeout}$	power output from thermal storage
P2G	power to gas
PV	photovoltaic
r_{leak}	thermal storage medium heat leakage rate
RMSE	root mean square error
$r_{parasitic}$	solar thermal electrical parasitic losses
sm	solar multiple
sv	final storage volume (m^3)
svi	effective required storage volume (m^3)
SWIS	south west interconnected system
TDR	total daily radiation (J/m^2)
$temp_{cold}$	cooled thermal storage medium temperature (°C)
$temp_{hot}$	heated thermal storage medium temperature (°C)
tl	line power loss over one grid link (%/1000km)
ts	design storage time (h)
tstep	simulation time step (h)
y	year

References

[1] W. Steffen, L. Hughes, A. Pearce, Climate change 2015: growing risks, critical choices, Climate Council of Australia, 2015.

[2] UNFCCC, Adoption of the Paris Agreement, (2015). https://unfccc.int/resource/docs/2015/cop21/eng/l09.pdf (accessed April 27, 2016).

[3] M. Springmann, D. Mason-D'Croz, S. Robinson, T. Garnett, H.C.J. Godfray, D. Gollin, M. Rayner, P. Ballon, P. Scarborough, Global and regional health effects of future food production under climate change: a modelling study, The Lancet. 387 (2016) 1937–1946. doi:10.1016/S0140-6736(15)01156-3.

[4] W.D. Gardiner, Analysis of the Technical Feasibility of Powering the South-West Interconnected System (SWIS) on 100% Renewable Energy, Masters Dissertation, Murdoch, 2013.

[5] M. Barrett, A renewable electricity system for the UK. A response to the 2006 energy review, (2006).

[6] J. Blackburn, Matching utility loads with solar and wind power in North Carolina dealing with intermittent electricity sources, Institute for Energy and Environmental Research, Takoma Park, USA, 2010. http://www.geni.org/globalenergy/library/technical-articles/generation/policy/eere/groundbreaking-study-finds/NC-Wind-Solar.pdf (accessed March 5, 2016).

[7] C. Budischak, D. Sewell, H. Thomson, L. Mach, D.E. Veron, W. Kempton, Cost-minimized combinations of wind power, solar power and electrochemical storage, powering the grid up to 99.9% of the time, J. Power Sources. 225 (2013) 60–74. doi:10.1016/j.jpowsour.2012.09.054.

[8] D. Connolly, H. Lund, B.V. Mathiesen, M. Leahy, The first step towards a 100% renewable energy-system for Ireland, Appl. Energy. 88 (2011) 502–507. doi:10.1016/j.apenergy.2010.03.006.

[9] D. Connolly, H. Lund, B.V. Mathiesen, Smart Energy Europe: The technical and economic impact of one potential 100% renewable energy scenario for the European Union, Renew. Sustain. Energy Rev. 60 (2016) 1634–1653. doi:10.1016/j.rser.2016.02.025.

[10] B. Elliston, M. Diesendorf, I. MacGill, Simulations of scenarios with 100% renewable electricity in the Australian National Electricity Market, Energy Policy. 45 (2012) 606–613. doi:10.1016/j.enpol.2012.03.011.

[11] M.Z. Jacobson, M.A. Delucchi, G. Bazouin, Z.A.F. Bauer, C.C. Heavey, E. Fisher, S.B. Morris, D.J.Y. Piekutowski, T.A. Vencill, T.W. Yeskoo, 100% clean and renewable wind, water, and sunlight (WWS) all-sector energy roadmaps for the 50 United States, Energy Env. Sci. 8 (2015) 2093–2117. doi:10.1039/C5EE01283J.

[12] S. Herbergs, H. Lehmann, S. Peter, The Computer-Modelled Simulation Of Renewable Electricity Networks, ISUSI, Institute for Sustainable Solutions and Innovations, Aachen, 2009.

[13] G. Hoste, M. Dvorak, M.Z. Jacobson, Matching Hourly and Peak Demand by Combining Different Renewable Energy Sources, VPUE Final Report, Stanford University, Palo Alto, California, 2009.

[14] H. Lehmann, Energy Rich Japan, Institute for Sustainable Solutions and Innovations (ISUSI), 2003.

[15] X. Luo, J. Wang, M. Dooner, J. Clarke, Overview of current development in electrical energy storage technologies and the application potential in power system operation, Appl. Energy. 137 (2015) 511–536. doi:10.1016/j.apenergy.2014.09.081.

[16] S. Weitemeyer, D. Kleinhans, T. Vogt, C. Agert, Integration of Renewable Energy Sources in future power systems: The role of storage, Renew. Energy. 75 (2015) 14–20. doi:10.1016/j.renene.2014.09.028.

[17] H. Lund, A.N. Andersen, P.A. Østergaard, B.V. Mathiesen, D. Connolly, From electricity smart grids to smart energy systems – A market operation based approach and understanding, Energy. 42 (2012) 96–102. doi:10.1016/j.energy.2012.04.003.

[18] B.V. Mathiesen, H. Lund, D. Connolly, H. Wenzel, P.A. Østergaard, B. Möller, S. Nielsen, I. Ridjan, P. Karnøe, K. Sperling, F.K. Hvelplund, Smart Energy Systems for coherent 100% renewable energy and transport solutions, Appl. Energy. 145 (2015) 139–154. doi:10.1016/j.apenergy.2015.01.075.

[19] B. Nastasi, G. Lo Basso, Hydrogen to link heat and electricity in the transition towards future Smart Energy Systems, Energy. 110 (2016) 5–22. doi:10.1016/j.energy.2016.03.097.
[20] S. Cheng, D. Xing, D.F. Call, B.E. Logan, Direct Biological Conversion of Electrical Current into Methane by Electromethanogenesis, Environ. Sci. Technol. 43 (2009) 3953–3958. doi:10.1021/es803531g.
[21] G. Guandalini, S. Campanari, M.C. Romano, Power-to-gas plants and gas turbines for improved wind energy dispatchability: Energy and economic assessment, Appl. Energy. 147 (2015) 117–130. doi:10.1016/j.apenergy.2015.02.055.
[22] M. Götz, J. Lefebvre, F. Mörs, A. McDaniel Koch, F. Graf, S. Bajohr, R. Reimert, T. Kolb, Renewable Power-to-Gas: A technological and economic review, Renew. Energy. 85 (2016) 1371–1390. doi:10.1016/j.renene.2015.07.066.
[23] W. Davis, M. Martín, Optimal year-round operation for methane production from CO2 and water using wind energy, Energy. 69 (2014) 497–505. doi:10.1016/j.energy.2014.03.043.
[24] J. Mullan, D. Harries, T. Bräunl, S. Whitely, Modelling the impacts of electric vehicle recharging on the Western Australian electricity supply system, Energy Policy. 39 (2011) 4349–4359. doi:10.1016/j.enpol.2011.04.052.
[25] Western Power, Ancillary Service Report 2013 prepared under clause 3.11.11 of the Market Rules by System Management, Western Power, Perth, 2013.
[26] IMOWA, 2014 Electricity Statement of Opportunities, Independent Market Operator Western Australia, Perth, 2015. http://www.imowa.com.au/docs/default-source/Reserve-Capacity/2014-electricity-statement-of-opportunities76EBFFC3E047.pdf (accessed September 16, 2015).
[27] IMO, Gas statement of opportunities, Independent Market Operator, Perth, 2015. www.imowa.com.au (accessed July 21, 2016).
[28] J. Riesz, S. Shiao, A. Turley, Assessment of FCS and Technical Rules, Roam Consulting, Brisbane, 2010.
[29] E.L. Da Silva, J.J. Hedgecock, J.C.O. Mello, J.C.F. Da Luz, Practical cost-based approach for the voltage ancillary service, Power Syst. IEEE Trans. On. 16 (2001) 806–812.
[30] S.T. Cha, H. Zhao, Q. Wu, A. Saleem, J. Østergaard, Coordinated control scheme of battery energy storage system (BESS) and distributed generations (DGs) for electric distribution grid operation, in: IECON 2012-38th Annu. Conf. IEEE Ind. Electron. Soc., IEEE, 2012: pp. 4758–4764. http://ieeexplore.ieee.org/xpls/abs_all.jsp?arnumber=6389587 (accessed December 17, 2015).
[31] A. Ulbig, T.S. Borsche, G. Andersson, Impact of low rotational inertia on power system stability and operation, ArXiv Prepr. ArXiv13126435. (2013). http://arxiv.org/abs/1312.6435 (accessed December 17, 2015).
[32] V. Knap, R. Sinha, M. Swierczynski, D.-I. Stroe, S. Chaudhary, Grid inertial response with Lithium-ion battery energy storage systems, in: Ind. Electron. ISIE 2014 IEEE 23rd Int. Symp. On, 2014: pp. 1817–1822. doi:10.1109/ISIE.2014.6864891.
[33] C. Rahmann, A. Castillo, Fast Frequency Response Capability of Photovoltaic Power Plants: The Necessity of New Grid Requirements and Definitions, Energies. 7 (2014) 6306–6322. doi:10.3390/en7106306.
[34] J.J. Vidal-Amaro, P.A. Østergaard, C. Sheinbaum-Pardo, Optimal energy mix for transitioning from fossil fuels to renewable energy sources – The case of the Mexican electricity system, Appl. Energy. 150 (2015) 80–96. doi:10.1016/j.apenergy.2015.03.133.
[35] P.J. Loftus, A.M. Cohen, J.C.S. Long, J.D. Jenkins, A critical review of global decarbonization scenarios: what do they tell us about feasibility?, Wiley Interdiscip. Rev. Clim. Change. 6 (2015) 93–112. doi:10.1002/wcc.324.
[36] P. Denholm, M. Mehos, Enabling greater penetration of solar power via the use of CSP with thermal energy storage, National Renewable Energy Laboratory, 2011.
[37] M. Liu, N.H. Steven Tay, S. Bell, M. Belusko, R. Jacob, G. Will, W. Saman, F. Bruno, Review on concentrating solar power plants and new developments in high temperature thermal energy storage technologies, Renew. Sustain. Energy Rev. 53 (2016) 1411–1432. doi:10.1016/j.rser.2015.09.026.
[38] B.V. Mathiesen, H. Lund, K. Karlsson, 100% Renewable energy systems, climate mitigation and economic growth, Appl. Energy. 88 (2011) 488–501. doi:10.1016/j.apenergy.2010.03.001.

[39] B. Elliston, I. MacGill, M. Diesendorf, Comparing least cost scenarios for 100% renewable electricity with low emission fossil fuel scenarios in the Australian National Electricity Market, Renew. Energy. 66 (2014) 196–204. doi:10.1016/j.renene.2013.12.010.
[40] J. Riesz, B. Elliston, Vithayasrichareon, Peerapat, MacGill, Ian, 100% Renewables for Australia?, Centre for Energy and Environmental Markets, University of NSW, Sydney, 2016. http://ceem.unsw.edu.au/sites/default/files/documents/100pc%20RE%20-%20Research%20Summary-2016-03-02a.pdf (accessed July 27, 2016).
[41] D. Laslett, C. Creagh, P. Jennings, A method for generating synthetic hourly solar radiation data for any location in the south west of Western Australia, in a world wide web page, Renew. Energy. 68 (2014) 87–102. doi:10.1016/j.renene.2014.01.015.
[42] D. Laslett, C. Creagh, P. Jennings, A simple hourly wind power simulation for the South-West region of Western Australia using MERRA data, Renew. Energy. 96 (2016) 1003–1014. doi:10.1016/j.renene.2016.05.024.
[43] ABS, 3218.0 - Regional Population Growth, Australia, 2013-14, Australian Bureau of Statistics, Canberra, 2015. http://www.abs.gov.au/AUSSTATS/abs@.nsf/Lookup/3218.0Main+Features12013-14?OpenDocument (accessed March 13, 2016).
[44] MR, Review of SWIS Planning Criterion, Market Research, 2012.
[45] N.B. Negra, J. Todorovic, T. Ackermann, Loss evaluation of HVAC and HVDC transmission solutions for large offshore wind farms, Electr. Power Syst. Res. 76 (2006) 916–927. doi:10.1016/j.epsr.2005.11.004.
[46] C.A. Dortolina, R. Nadira, The Loss That is Unknown is No Loss At All: A Top-Down/Bottom-Up Approach for Estimating Distribution Losses, IEEE Trans. Power Syst. 20 (2005) 1119–1125. doi:10.1109/TPWRS.2005.846104.
[47] A.S. Masoum, S. Deilami, P.S. Moses, A. Abu-Siada, Impacts of battery charging rates of plug-in electric vehicle on smart grid distribution systems, in: Innov. Smart Grid Technol. Conf. Eur. ISGT Eur. 2010 IEEE PES, IEEE, 2010: pp. 1–6. http://ieeexplore.ieee.org/xpls/abs_all.jsp?arnumber=5638981 (accessed September 24, 2015).
[48] M.P. Bahrman, HVDC transmission overview, in: Transm. Distrib. Conf. Expo. 2008 T X00026 IEEEPES, IEEE, 2008: pp. 1–7. http://ieeexplore.ieee.org/xpls/abs_all.jsp?arnumber=4517304 (accessed September 24, 2015).
[49] E. Koutroulis, F. Blaabjerg, Design Optimization of Transformerless Grid-Connected PV Inverters Including Reliability, IEEE Trans. Power Electron. 28 (2013) 325–335. doi:10.1109/TPEL.2012.2198670.
[50] A.. Carr, T.. Pryor, A comparison of the performance of different PV module types in temperate climates, Sol. Energy. 76 (2004) 285–294. doi:10.1016/j.solener.2003.07.026.
[51] T. Huld, R. Gottschalg, H.G. Beyer, M. Topič, Mapping the performance of PV modules, effects of module type and data averaging, Sol. Energy. 84 (2010) 324–338. doi:10.1016/j.solener.2009.12.002.
[52] B. Jones, N. Wilmot, A. Lark, Study on the impact of Photovoltaic (PV) generation on peak demand, Network. (2012). http://pdc-cmsdgp02.westernpower.com.au/documents/Photovoltaic_Forecast_Public_Version_2012.pdf (accessed August 28, 2015).
[53] APVI, Australian PV Institute (APVI) Solar Map, funded by the Australian Renewable Energy Agency, (2016). pv-map.apvi.org.au (accessed March 14, 2016).
[54] ABS, 2011 Census QuickStats Greater Perth, Australian Bureau of Statistics, Perth, 2011. http://www.censusdata.abs.gov.au/census_services/getproduct/census/2011/quickstat/5GPER?opendocument&navpos=220 (accessed April 8, 2013).
[55] DIT, State of Australian cities 2012., Infrastructure Australia, Department of Infrastructure and Transport Major Cities Unit, Canberra, ACT, 2012.
[56] Y. Tian, C.Y. Zhao, A review of solar collectors and thermal energy storage in solar thermal applications, Appl. Energy. 104 (2013) 538–553. doi:10.1016/j.apenergy.2012.11.051.
[57] M.J. Wagner, Simulation and predictive performance modeling of utility-scale central receiver system power plants, University of Wisconsin–Madison, 2008.

[58] C.E. Tyner, D. Wasyluk, eSolar's modular, scalable molten salt power tower reference plant design, in: 19th Annu. SolarPACES Symp., 2013. http://www.esolar.com/wp-content/uploads/2013/10/SolarPACES-2013.pdf (accessed March 14, 2016).
[59] J. Hinkley, B. Curtin, J. Hayward, A. Wonhas, R. Boyd, C. Grima, A. Tadros, R. Hall, K. Naicker, A. Mikhail, Concentrating solar power–drivers and opportunities for cost-competitive electricity, Clayton South CSIRO. (2011). https://publications.csiro.au/rpr/download?pid=csiro:EP111647&dsid=DS3 (accessed September 14, 2015).
[60] M.M. Rienecker, M.J. Suarez, R. Gelaro, R. Todling, J. Bacmeister, E. Liu, M.G. Bosilovich, S.D. Schubert, L. Takacs, G.-K. Kim, others, MERRA: NASA's modern-era retrospective analysis for research and applications, J. Clim. 24 (2011) 3624–3648.
[61] G.L. Soloveichik, Battery Technologies for Large-Scale Stationary Energy Storage, Annu. Rev. Chem. Biomol. Eng. 2 (2011) 503–527. doi:10.1146/annurev-chembioeng-061010-114116.
[62] B.D. McCloskey, Expanding the Ragone Plot: Pushing the Limits of Energy Storage, J Phys Chem Lett. 6 (2015) 3592–3593.
[63] A. Mishra, R. Sitaraman, D. Irwin, T. Zhu, P. Shenoy, B. Dalvi, S. Lee, Integrating Energy Storage in Electricity Distribution Networks, in: ACM Press, 2015: pp. 37–46. doi:10.1145/2768510.2768543.
[64] M. Jentsch, T. Trost, M. Sterner, Optimal Use of Power-to-Gas Energy Storage Systems in an 85% Renewable Energy Scenario, Energy Procedia. 46 (2014) 254–261. doi:10.1016/j.egypro.2014.01.180.
[65] R.A. Alvarez, S.W. Pacala, J.J. Winebrake, W.L. Chameides, S.P. Hamburg, Greater focus needed on methane leakage from natural gas infrastructure, Proc. Natl. Acad. Sci. 109 (2012) 6435–6440.
[66] S. Backlund, P. Thollander, J. Palm, M. Ottosson, Extending the energy efficiency gap, Energy Policy. 51 (2012) 392–396.
[67] S. Nadel, A. Shipley, R.N. Elliott, The technical, economic and achievable potential for energy-efficiency in the US–A meta-analysis of recent studies, in: Proc. 2004 ACEEE Summer Study Energy Effic. Build., 2004: pp. 8–215.
[68] K.J. Chua, S.K. Chou, W.M. Yang, J. Yan, Achieving better energy-efficient air conditioning – A review of technologies and strategies, Appl. Energy. 104 (2013) 87–104. doi:10.1016/j.apenergy.2012.10.037.
[69] H.G. Huntington, The policy implications of energy-efficiency cost curves, Energy J. 32 (2011) 7–22.
[70] REN21, Renewables 2016 Global Status Report, REN21 Secretariat, Paris, 2016.
[71] AWDC, Perth snapshot 2011, Aboriginal workforce development centre. Government of Western Australia department of training and workforce development, Perth, 2011. http://www.dtwd.wa.gov.au/employeesandstudents/aboriginalworkforcedevelopmentcentre/resources/regional-snapshots/Documents/Final%20Perth%20Snapshot%202011%20V1%202.pdf (accessed June 11, 2015).
[72] IRENA, Battery storage For renewables: Market status And technology Outlook, 2015.
[73] M.G. Hughes, A.D. Heap, National-scale wave energy resource assessment for Australia, Renew. Energy. 35 (2010) 1783–1791. doi:10.1016/j.renene.2009.11.001.
[74] H. Wu, Q. Fu, R. Giles, J. Bartle, Production of Mallee Biomass in Western Australia: Energy Balance Analysis †, Energy Fuels. 22 (2008) 190–198. doi:10.1021/ef7002969.
[75] P. Hearps, R. Dargaville, D. McConnell, M. Sandiford, P. Seligman, Opportunities for Pumped Hydro Energy Storage in Australia, Melbourne Energy Institute, Melbourne, 2014.
[76] C. Turchi, M. Mehos, C.K. Ho, G.J. Kolb, Current and future costs for parabolic trough and power tower systems in the US market, SolarPACES 2010. (2010). http://www.nrel.gov/docs/fy11osti/49303.pdf (accessed June 2, 2016).
[77] C. Singer, R. Buck, R. Pitz-Paal, H. Müller-Steinhagen, Assessment of solar power tower driven ultrasupercritical steam cycles applying tubular central receivers with varied heat transfer media, J. Sol. Energy Eng. 132 (2010) 041010.
[78] P. Gauché, S. Pfenninger, A.J. Meyer, T.W. von Backström, A.C. Brent, Modeling dispatchability potential of CSP in South Africa, SASEC 2012. (2012). http://concentrating.sun.ac.za/wp-content/uploads/2012/07/PL-03.pdf (accessed April 7, 2016).

[79] M.J. Wagner, G. Zhu, A generic CSP performance model for NREL's System Advisor Model, in: Proc. 17th SolarPACES Symp. Granada Spain, 2011. http://www.nrel.gov/docs/fy11osti/52473.pdf (accessed April 16, 2016).

[80] J.W. Spencer, Perth solar tables: tables for solar position and radiation for Perth (latitude 32.0° S.) in SI units, Commonwealth Scient. and Industrial Research Org, Melbourne, 1976.

[81] A.L. Avila-Marin, J. Fernandez-Reche, F.M. Tellez, Evaluation of the potential of central receiver solar power plants: Configuration, optimization and trends, Appl. Energy. 112 (2013) 274–288. doi:10.1016/j.apenergy.2013.05.049.

[82] S.H. Madaeni, R. Sioshansi, P. Denholm, How Thermal Energy Storage Enhances the Economic Viability of Concentrating Solar Power, Proc. IEEE. 100 (2012) 335–347. doi:10.1109/JPROC.2011.2144950.

[83] R. Bayón, E. Rojas, Simulation of thermocline storage for solar thermal power plants: From dimensionless results to prototypes and real-size tanks, Int. J. Heat Mass Transf. 60 (2013) 713–721. doi:10.1016/j.ijheatmasstransfer.2013.01.047.

[84] P. Denholm, Y.-H. Wan, M. Hummon, M. Mehos, An analysis of concentrating solar power with thermal energy storage in a California 33% renewable scenario, Contract. 303 (2013) 275–3000.

1. 100% renewable electricity simulation developed for the south west of Western Australia.
2. Balancing supply and demand is tough: grid is isolated and no pumped hydro capacity.
3. Solar PV, solar thermal, wind farms, battery storage, P2G and energy efficiency used.
4. Generic solar thermal power tower two tank thermal storage model developed.
5. Grid inertia maintained, supply and demand balanced hour by hour throughout year.

Response to review comments

Ms. Ref. No.: RENE-D-16-03430
Title: A large-scale renewable electricity supply system by 2030: solar, wind, energy efficiency, storage and inertia for the South West Interconnected System (SWIS) in Western Australia.

Renewable Energy

Reviewers' comments (in bold type) and responses:

Reviewer #1: The article is interesting and fits for Journal's topic.
Two main flaws must faced by the authors:

- since you performed simulations a proper error analysis is required to understand the quality of your outcome and the error related to each assumption.

Error analysis for the solar and wind models was done in previous papers. For solar irradiance, a sentence will be added in this paper:

"The average Mean Bias Error (MBE) between the synthetic and measured irradiance falling on a horizontal plane was found to be -0.81%, indicating slightly conservative synthetic values. The monthly averaged irradiance Root Mean Square Error (RMSE) was 10.5%."

For wind power, a sentence will be added in this paper:

"The average MBE between the yearly synthetic and measured values was -4.6%, and the average RMSE was 9.4%."

Error analysis for the solar thermal with storage model was already reported in this paper:

"The model was calibrated to the power tower model used in the System Advisor Model (SAM)(Wagner 2008), such that the power output Root Mean Square Error (RMSE) compared to SAM was less than 25%, and the stored energy RMSE was less than 10%. The overall solar to electric efficiency for a power tower with 15 hours storage was around 14.5%, slightly below the value of 15.8% predicted by Tyner and Wasyluk (2013) for a power tower with 13 hours of storage, but close to the value of 14.6% modelled by Hinckley et al. (2011) for a power tower with 6 hours of storage using SAM. Hence the solar thermal model used in this study is slightly conservative."

Thus values for energy generation were slightly conservative, meaning that the estimated required capacity for each technology in the scenarios to balance supply with demand might be slightly higher than needed.

- some key literature is missing, starting from the one published in this Journal as well as the articles published in other high-quality Journals, please include in your study:
http://www.sciencedirect.com/science/article/pii/S0960148115302032
http://www.sciencedirect.com/science/article/pii/S0360544216303413
http://www.sciencedirect.com/science/article/pii/S1364032116002331
http://www.sciencedirect.com/science/article/pii/S0360319916315063
http://www.sciencedirect.com/science/article/pii/S1364032116311716

Reference [10] in the paper covers 100% renewable energy scenarios for 50 of the states in the US. Hence reference [10] is more comprehensive than the suggested reference Jacobson et al. (2016) (S0960148115302032), which only covers the state of Washington. Both papers are based on the same modelling, so it seems unnecessary to include this extra reference.

Article by Nastasi and Lo Basso (2016) (S0360544216303413) added to citations.
Article by Connolly et al. (2016) (S1364032116002331) added to citations.

Articles by Uyar and Besikci (2017) (S0360319916315063) and Akuru et al. (2017) (S1364032116311716) not added because they do not appear to include or cite modelling for energy balance between supply and demand on an hourly time scale for the whole electrical demand of the countries studied.

The reviewer considers a positive outcome of the process if those measures will be adopted.

Reviewer #2: 1- Generally Hybrid models using Homier software, etc. has been used to predict the best method for electricity generation - wind, solar, bio-gas etc. How it is different as is compared to your model to?

The design tool developed in this study was designed to allow interactive operation, and accessibility, and the ability to work off line. Hence, it was developed using Javascript and dynamic HTML, languages which most modern browsers recognise, and most modern computers will have a web browser. The design tool simulates a large scale grid with multiple wind farms and solar power plants. These wind farms and power plants can be sited anywhere within the south west of Western Australia. Hourly wind speed or solar irradiance data will be automatically generated for each particular site.

Additionally, the wind power model developed here was designed to take into account the output power spatial correlation between multiple wind farms sited close together.

In contrast, Homer is now commercial non-free software, so general accessibility is reduced. Homer was designed to simulate micro power systems, and is usually applied to small scale systems with a single wind turbine, so that taking spatial correlation into

account is not required. Homer requires the user to provide hourly wind speed and/or solar radiation data for each site. Synthetic hourly wind speed or solar irradiance data can be generated by Homer, but some longer time scale averaged values must still be provided (usually monthly).

2- Is your model going to be operated as an independent power since it is not associated with connection other grids?

Yes, the SWIS is a large electrical grid, but it is isolated, so all electrical power generation scenarios will operate independently. The isolation is one of the factors that make the SWIS an interesting case study, relevant to other isolated grids. This was already stated in the abstract and introduction.

3- Can you give a brief description of the 2050 target as compared to your 2030 model? States the merits and demerit associated with the models?

The following paragraph will be added:

"If the target was delayed until 2050, more capacity may be required to meet increased demand (assuming population growth continues at the same rate), but there is also more time to gain further energy efficiency improvements, solar PV cell efficiencies are likely to increase further, perhaps wind turbine capacity factors will be greater, and there is more time to build the required capacity, so the build schedule would be more relaxed than the 2030 target. The cost of many of the technologies discussed here are falling, so they may be even cheaper by 2050. A fully renewable energy system may be built well before 2050 for purely financial reasons. An unknown factor would be that climate change may have affected the wind patterns across the SWWA to a greater extent and also the solar radiation patterns. Although an electrical system based more on distributed generation and storage could be expected to be more resilient, aiming for a 2030 target to avoid the increased risk of disruptive extreme weather events from dangerous climate change is preferable."

4- Authors must come up with the real descriptions for the model of SWIS, for instance what type of equipment/ software were used to generate the results? A description diagram or figure as discussed in appendix A could be a great help in understand the model.

The model of the SWIS grid was already described in the 'Transmission losses' subsection within the method section. The authors developed their own model of the SWIS, consisting of main transmission lines (Figure 2), and extra local connections to new power stations. The load centre was assumed to be based on Perth. Transmission line losses for every large scale power station were estimated using equation 3. Distributed solar PV and storage within the SWIS network were assumed to have conversion losses.